Journal of
Composites Science

MDPI

Review

4D-Printed Liquid Crystal Elastomers: Printing Strategies, Actuation Mechanisms, and Emerging Applications

Mehrab Hasan and Yingtao Liu *

School of Aerospace and Mechanical Engineering, The University of Oklahoma, Norman, OK 73019, USA; mehrab.hasan-1@ou.edu
* Correspondence: yingtao@ou.edu

Abstract

Liquid crystal elastomers (LCEs), as a class of smart materials, have attracted significant attention across soft robotics, biomedical engineering, and intelligent devices because of their unique capabilities to undergo large, reversible, and anisotropic deformations under external stimuli. Over the years, fabrication methods have advanced from conventional molding and thin-film processing to additive manufacturing, with 4D printing emerging as a transformative approach by enabling time-dependent, programmable shape transformations. Among the available methods, direct ink writing (DIW) and vat photopolymerization are most widely adopted, with ink chemistry, rheology, curing, and printing parameters directly governing mesogen alignment and actuation performance. Recent advances in LCE actuators have demonstrated diverse functionalities in soft robotics, including bending, crawling, gripping, and sequential actuation, while biomedical applications span adaptive tissue scaffolds, wearable sensors, and patient-specific implants. This review discusses the conceptual distinction between 3D and 4D printing, compares different additive manufacturing techniques for LCE, and highlights emerging applications in the field of soft robotics and biomedical technologies. Despite rapid progress in LCE, challenges remain in biocompatibility, long-term durability and manufacturing scalability. Overall, innovations in 4D printing of LCEs underscores both the promise and the challenges of these materials, pointing toward their transformative role in enabling next-generation soft robotic and biomedical technologies.

Keywords: liquid crystal elastomer; 4D printing; DIW; vat photopolymerization; actuators; soft robotics; biomedical technology

check for updates

Academic Editor: Jacob Aboudi

Received: 10 October 2025
Revised: 8 November 2025
Accepted: 9 November 2025
Published: 13 November 2025

Citation: Hasan, M.; Liu, Y. 4D-Printed Liquid Crystal Elastomers: Printing Strategies, Actuation Mechanisms, and Emerging Applications. *J. Compos. Sci.* **2025**, *9*, 633. https://doi.org/10.3390/jcs9110633

Copyright: © 2025 by the authors. Licensee MDPI, Basel, Switzerland. This article is an open access article distributed under the terms and conditions of the Creative Commons Attribution (CC BY) license (https://creativecommons.org/licenses/by/4.0/).

1. Introduction

Liquid crystal elastomers (LCEs) can be defined as stimuli-responsive polymers which are capable of large, reversible, and anisotropic shape changes under thermal, optical, or other stimuli [1–3].Their unique properties arise from the coupling of the orientational order of liquid-crystal mesogens with the elasticity of lightly cross-linked polymer networks [4,5]. Research at the very initial stage anticipated an elastic solid with internal nematic order, and the first LCEs were realized in the 1980s when Finkelmann et al. cross-linked liquid-crystalline polymers into elastic networks. Their two-step crosslinking produced monodomain LCEs with globally aligned mesogens [6]. These breakthroughs established LCEs as "smart" polymer actuators, advancing research into applications such as artificial muscles and soft actuators in robotics and biomedical devices [7].

In this broader framework, the 4D Printing Roadmap by Bodaghi et al. provides a comprehensive vision for the evolution of additive manufacturing, emphasizing how smart materials are advancing from single-function to programmable, time-responsive systems [8]. Within this roadmap, shape-memory polymers (SMPs) are identified as the foundational class that introduced the principle of encoded shape recovery, which marked the onset of 4D printing. Building upon that conceptual base, (LCEs) represent the next evolutionary step: combining anisotropic molecular alignment with reversible actuation to overcome the one-way limitations of SMPs. Earlier fabrication methods used to produce thin films or uniformly aligned sheets, thus limiting deformation to extension or contraction only. 4D printing extends conventional 3D printing by incorporating stimulus-responsive materials: instead of manufacturing static objects layer by layer, it adds a time dimension so that printed structures can alter shape or function in response to the applied stimuli [9]. In LCEs, this derives from the nematic–isotropic phase transition: mesogens are aligned and cross-linked during printing; heating causes contraction along the director, and cooling restores the shape. Early 4D-printed LCEs utilized temperature gradients during printing to create orientation gradients within each filament, resulting in bending, twisting, and linear actuation [10]. Later approaches go on to decouple printing and shape programming, enabling more complex architecture.Figure 1 provided a overall schematic of the entire 4D printing processes and applications.

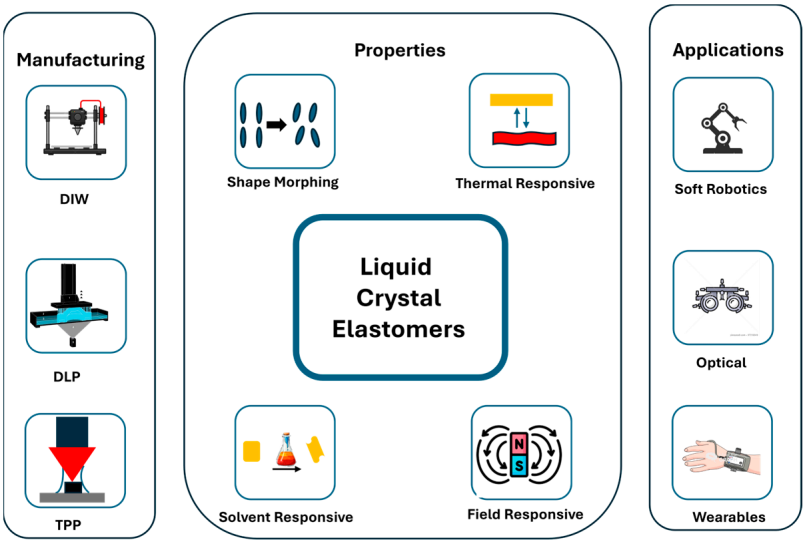
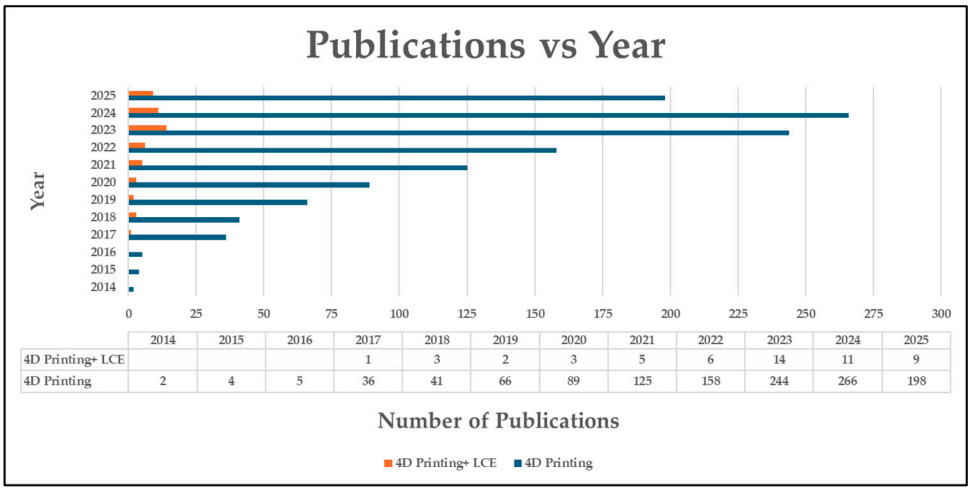


Figure 1. Schematic diagram of 4D printing of Liquid crystal elastomers (LCEs), applications, and properties.

4D printing greatly expands the design space for LCE actuators compared to conventional fabrication methods in existence. It enables spatial control of mesogen alignment and the creation of complex 3D architectures that were unattainable by casting. Multi-material printing allows rigid fibers or passive polymers to be embedded within an LCE matrix, and by adjusting parameters like local orientation gradients, print speed, and cross-linking sequence, researchers can tune actuation strain, stress, energy dissipation, and sequential deformations [11,12]. The resulting actuators display bending, twisting, folding, and multistep motions, which are beyond the one-dimensional actuation of simple LCE films. These capabilities help to enable sophisticated applications across multiple scales. At the centimeter scale, LCE-based actuators exhibit lifelike motion under thermal or optical stimulation. By programming the local alignment of mesogens, a single part can bend, curl, twist, or oscillate sequentially. At micro- and sub-micrometer scales, one of the 4D printing techniques, two-photon polymerization (TPP), has produced LCE micro-

actuators for adaptive optics, micromechanics, and tunable photonic structures [13]. 4D printing, combined with dynamic covalent chemistry, yields self-healing, reprogrammable actuators [13]. The ability to program shape changes in both dry and wet environments makes LCEs attractive for biomedical applications, such as tissue engineering scaffolds, minimally invasive tools, and wearable therapeutic devices. LC-based biosensors are laying the foundation for research in LCE-based biosensing techniques, although it is still in its early stages of development [14,15].

To gain an understanding of how 4D printing influences the advanced manufacturing process worldwide, a bibliographic search was conducted using the Scopus database, spanning from 2014 to October 2025. Only peer-reviewed published articles containing the keyword "4D printing" were considered for this analysis. However, if the keywords "4D printing" and "Liquid Crystal Elastomer" are considered, then it reflects that this specific domain of research, which integrates 4D printing with the manufacturing of LCEs, is emerging, and there is immense potential for further research on diversified interests. During the last 10 years, since the first application of 4D printing, research has progressed by 10-folds as shown in Figure 2. However, when it comes to works that incorporate both 4D printing techniques and the manufacturing of LCEs, the number of publications is significantly lower than the broader scope. Even in 2025, it is still less than one-twentieth of the total number of publications related to 4D printing. Hence, it is evident that there is sufficient scope for this field to grow and novel ideas to be introduced.



	2014	2015	2016	2017	2018	2019	2020	2021	2022	2023	2024	2025
4D Printing+ LCE				1	3	2	3	5	6	14	11	9
4D Printing	2	4	5	36	41	66	89	125	158	244	266	198

Figure 2. 4D printing publications trend over the period (2014–2025) and comparison between keywords—"4D Printing" only and "4D printing + LCE", based on Scopus database.

Table 1 provides an overview of the global 4D printing research landscape and identifies the most significant contributors over the years from 2014 to 2025. China occupied the leading position in this sector, with 507 peer-reviewed articles published during this period, more than double the number of articles published by the second-place country, the USA (207 articles). Among European countries, the UK is the highest contributor in this sector. India and Singapore are also advancing 4D printing research around Asia. This table outlines how the manufacturing infrastructure is expected to evolve in the future by integrating 4D printing globally and identifies the leading inventors. Major contributing affiliations of the top ten countries were also listed to gain an understanding of how research has progressed globally and across various institutions.

Table 1. Most contributing countries and leading affiliations from those countries based on the Scopus Database during the period (2014–2025).

Country/Territory	Number of Publications	Most Contributing Affiliations	Number of Publications
China	507	Ministry of Education of the People's Republic of China	77
United States	211	Georgia Institute of Technology	40
United Kingdom	132	Nottingham Trent University	59
India	87	National Institute of Technical Teachers Training & Research	11
Singapore	67	Nanyang Technological University	39
Germany	61	Universität Heidelberg	11
France	60	CNRS Centre National de la Recherche Scientifique	28
Iran	59	University of Tehran	34
South Korea	57	Seoul National University	14
Australia	52	Deakin University	26

In light of the rapid advances in this field, the motivation for this review is to examine the most recent developments in 4D-printed LCE actuators and discuss their applications, with a focus on soft robotics and biomedical technology. We begin by introducing the material synthesis strategies used to prepare LCEs suitable for 4D printing, including formulations and alignment techniques that would enable programmable shape change. This section also examines how alignment and shape programming of LCEs are achieved, covering methods to orient liquid crystal domains by applying techniques such as mechanical stretching, magnetic or electric fields, and shear alignment during printing, as well as methods to fix programmed shapes via curing. In the next section, an overview of the additive manufacturing techniques employed for the 4D printing of LCEs is provided, emphasizing primary techniques such as direct ink writing and vat photopolymerization. The section also describes how processing conditions influence mesogen alignment and actuation behavior. Following this, the typical actuation behaviors and performance metrics of 4D-printed LCE actuators are discussed, highlighting improvements in reversible strain output, response times, and multimodal deformation compared to conventionally manufactured LCEs. Finally, a range of emerging applications of 4D-printed LCE technology, from soft robotic devices such as grippers and artificial muscles to locomotion robots and biomedical applications, including tissue-engineering scaffolds, smart medical implants, and wearable sensors, are analyzed. The conclusion outlines current challenges and future opportunities for LCE-based soft actuators in these areas.

2. Synthesis and Shape Programming of LCE

2.1. Fundamentals of Liquid Crystal Elastomers

As a shape-morphing material, LCEs combine the elastic properties of rubber with the anisotropic, stimuli-responsive characteristics of liquid crystals (LCs) with synergy [16]. This specific structure allows LCEs to undergo significant, reversible shape changes when exposed to external stimuli such as heat, light, or electric and magnetic fields. This concept was first predicted over 50 years ago by Pierre-Gilles de Gennes, who envisioned that polymeric materials retaining liquid crystallinity would exhibit a significant stimulus response comparable to the cooperative expansile–contractile response of a muscle fiber [17]. The subsequent synthesis of these materials confirmed his predictions, establishing LCEs as a compelling field of research for applications ranging from soft robotics and optics [18] to healthcare [19] and consumer goods [20].

The LCE unit structure consists of a lightly cross-linked polymer network into which rigid, rod-like mesogens are integrated [21]. These mesogens can be incorporated either directly into the polymer backbone (main-chain LCEs) or attached as pendant-like shapes via flexible spacers (side-chain LCEs), as illustrated in Figure 3. The intermolecular interactions between these mesogens (e.g., π-stacking, dipole–dipole interactions) are retained within the polymer network, which allows the formation of liquid crystalline phases, commonly referred to as the nematic phase. A critical distinction in LCEs is their macroscopic mesogen alignment. Without an aligning field during synthesis, the mesogens form randomly oriented, localized domains, resulting in a polydomain LCE. It does not undergo significant, coherent shape changes upon activation [22]. To achieve the large-scale, cooperative actuation, a global, uniform alignment must be imparted, creating a monodomain LCE where the mesogens are collectively oriented along a single director, n [21].

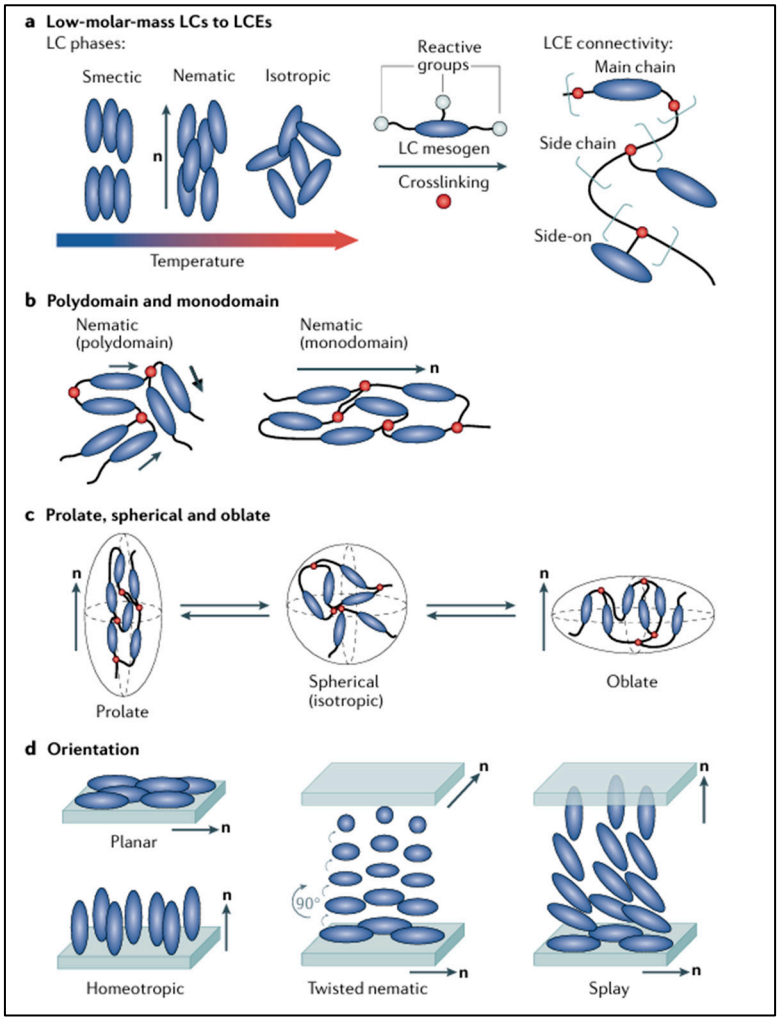


Figure 3. Detailed demonstration of side-chain and main-chain architectures for LCEs, the definition of the nematic order parameter, and how actuation arises from the nematic–isotropic transition. Reproduced with permission from Springer Nature [7].

An order-disorder phase transition drives the actuation mechanism of a monodomain LCE. In its nematic, i.e., ordered state, the polymer chains adopt an anisotropic conformation, generally a prolate (elongated) ellipsoid. When a stimulus like heat is applied, the orientational order of the mesogens is disrupted, causing the polymer chains to transition to a more disordered, spherical configuration [7]. This microscopic variation in chain conformation translates into a macroscopic contraction along the director n and consequently

an expansion happens in perpendicular directions. This reversible strain can be substantial, with deformations up to the level of 400% reported for thermally responsive LCEs [23]. The process is fully reversible when stimulus is removed, since the elastic memory of the cross-linked network re-establishes the original network configuration and mesogen order [22]. This large-strain response is a key feature that distinguishes LCEs from more densely cross-linked and glassy liquid crystalline networks (LCNs), which exhibit actuation strains of 5% or less due to their limited polymer chain mobility [7].

Although LCEs and shape-memory polymers (SMP) are both stimuli-responsive polymer networks, their mechanisms and material properties are different in some fundamental aspects. LCEs integrate orientationally ordered mesogen units within an elastomeric network on a nematic-to-isotropic transition, which is triggered by heat, light or electric field. The mesogens could lose alignment, causing anisotropic contraction along the original director and expansion perpendicular to it. Hence they would enable large, reversible deformations tied to liquid-crystalline order and rubber elasticity [24]. In contrast, SMPs consist of cross-linked networks with permanent net-points and distinct switching domains (e.g., segments above Tg or Tm): the material is deformed into a temporary shape when the switching domain is soft, fixed upon cooling, and then recovers its original shape upon reheating thanks to the stored entropic elasticity of the network [25,26].

Although both classes rely on cross-linked polymeric networks and exhibit large strain responses to stimuli, LCEs are inherently anisotropic and rely on the coupling of mesogenic orientation and network deformation, enabling reversible actuation [27], while SMPs are largely isotropic, dependent on shape-fixing and recovery mechanisms, and generally exhibit one-way shape change unless engineered specifically [26]. From a structural viewpoint, LCEs represent liquid-crystalline phase behavior embedded in elastomeric matrices [24], whereas SMPs utilize phase transitions (glass or melt) of switching segments embedded in an elastic matrix [26]. These intrinsic distinctions shape their mechanical responses, reversibility, and design strategies in smart polymer systems.

2.2. Synthesis of LCEs

The synthesis of functional LCEs is intrinsically linked to alignment of mesogens before the polymer network is permanently fixed [22]. Several chemical strategies have been developed to achieve this, often involving multistep or dynamic reaction schemes to accommodate different alignment techniques. However, there can be practical obstacle to implement synthesis strategies. For example, thermally induced polymerizations often require solvents to ensure reactant mobility, but undesirable deswelling and deformation can happen for the subsequent removal of these solvents. Conversely, photocuring with UV light helps to avoid high temperatures but is limited to thin samples (several hundred micrometers) due to the limited penetration depth of light [28]. Different synthesis processes are demonstrated in Figure 4.

"Finkelmann method" is one of the pioneering synthesis reactions. It involves a two-step hydrosilylation process where a partially cross-linked polysiloxane network is formed first [6]. This network is then mechanically stretched to align the mesogens. Then, the polymerization is completed to lock in the monodomain structure. This approach typically relies on kinetic differences between two crosslinkers: the faster-reacting one forming the initial weak network and the slower one completing the reaction under load [7].

Recently, chain-extension reactions have gained popularity due to their use of commercially available materials. These type of reactions are also compatible with a broader range of alignment methods [7]. Among them, aza-Michael addition enables diacrylate LC monomers to react with primary amines and form oligomers that are subsequently photopolymerized. The low initial viscosity and slow kinetics of this reaction make it a

suitable option for surface-enforced alignment [29]. Similarly, thiol-Michael addition [30] and thiol-ene reactions [29] are used to create LCEs from readily available precursors, offering accessible and versatile routes to programmable materials.

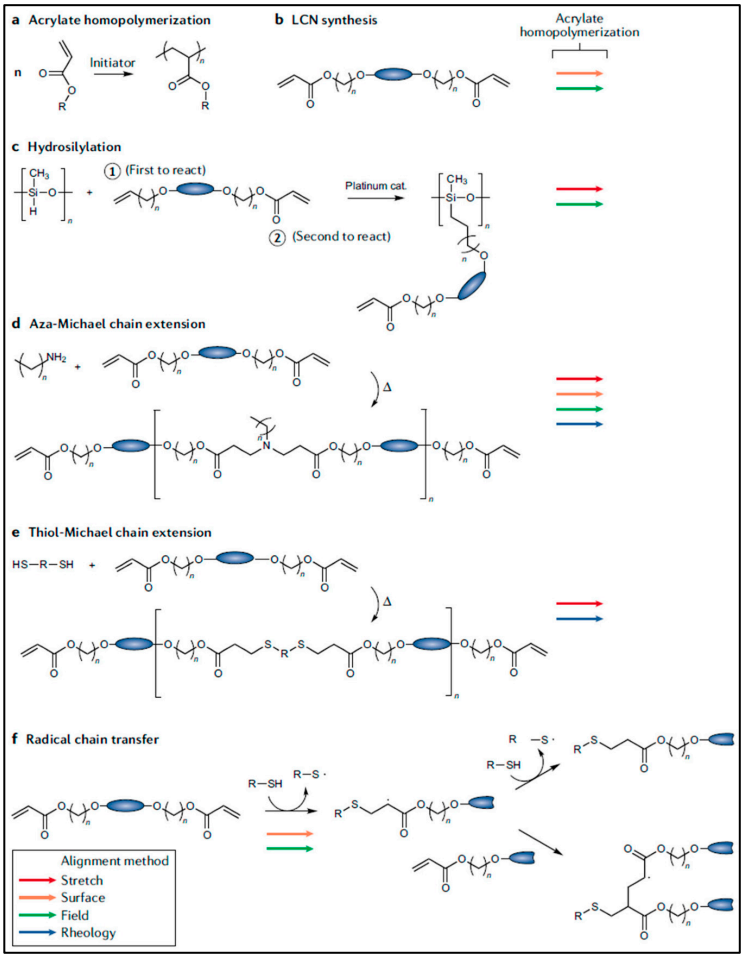


Figure 4. Synthetic approaches for the preparation of crosslinked liquid crystalline polymers: (**a**) A photoinitiated acrylate homopolymerization to prepare LCNs (**b**) Synthesis of LCNs, (**c**) Aligned liquid crystalline elastomers are prepared by the two-step 'Finkelmann method', comprising a platinum-catalyzed hydrosilylation, and followed by a photoinitiated radical crosslinking polymerization, (**d**) aza-Michael oligomerization and successive photo, (**e**) thiol-Michael chain extension and subsequent crosslinking photopolymerization of residual groups (stretch and rheological alignment), and (**f**) a radical chain transfer reaction (surface and field alignment). Reproduced with permission from Springer Nature [7].

The direct ink writing printable LCE inks are generally synthesized by applying aza-Michael or thiol-Michael addition reactions. Formulation steps are as follows: (1) bifunctional reactive mesogens forming the polymer backbone, (2) chain extenders or isotropic cross-linkers tuning cross-link density, (3) photoinitiators to trigger curing, and (4) catalysts accelerating thermal reactions. Thiol-Michael chemistry is essential in 4D printing of LCEs, since it provides precise control of the nematic–isotropic transition temperature (TNI), cross-link density, and overall actuation performance. These chemical routes give researchers fine control over rheology and curing kinetics, ensuring the printability of the ink while enabling the desired mechanical and thermal properties [31–33].

An emerging synthetic approach involves Dynamic Covalent Chemistry (DCC), which incorporates reversible covalent bonds, such as disulfide, boronic esters, or those involved in transesterification, into the LCE network [34]. Applying DCC, a polydomain LCE can be

synthesized in a single step and then reprogrammed. By applying a stimulus like heat or light to dissociate the dynamic bonds, the mesogens can be mechanically realigned, and upon removal of the stimulus, the bonds reform, fixing the new orientation [7]. This method not only facilitates alignment but also imparts desirable properties such as reprocessability, self-healing, and the ability to weld material pieces together [35–37], greatly improving the material's versatility and applicability. This reprogrammability is significant since it overcomes the limitation of being fixed to a single programmed geometry by allowing the final actuated shape to be modified as needed.

2.3. Orientation and Shape Programming Mechanism

During material synthesis, LC alignment is programmed, and it dictates the complexity level of actuation. This is an essential step since it involves creating a specific mesogen orientation (director profile) before full cross-linking of the polymer network, thereby predetermining the material's shape-morphing behavior [22]. The process is accomplished in three steps: (1) partial crosslinking to create an elastic network of orientable polymer chains, (2) applying an orientational field (e.g., mechanical stress) to align the mesogens into the desired or required configuration, and (3) a final crosslinking step to permanently preserve the aligned network topology, as shown in Figure 3. Shape programming ensures that the same structure is reestablished after each stimulus, enabling consistent and reversible shape variation.

By programming non-uniform director profiles, complex 3D shape transformations can be constructed from 2D sheets. For instance, a simple uniaxial alignment can result in linear contraction, while through-thickness transformations, such as twisted nematic or splayed alignments, can create bending and twisting actuations. Applying stimulation, more sophisticated patterns, such as an azimuthal director profile with a + 1 topological defect, can program a flat sheet to morph into a 3D cone. While traditional shape programming inhibits the material from morphing between its initial and programmed shapes, techniques such as fusing differently programmed LCE pieces or utilizing dynamic bonds for reprogramming are expanding the versatility and complexity of achievable shape changes [37]. For example, using a photomask during photo-crosslinking as shown in Figure 5, regions of aligned and non-aligned materials are patterned within a single sample, creating internal mechanical inhomogeneities that drive complex deformations.

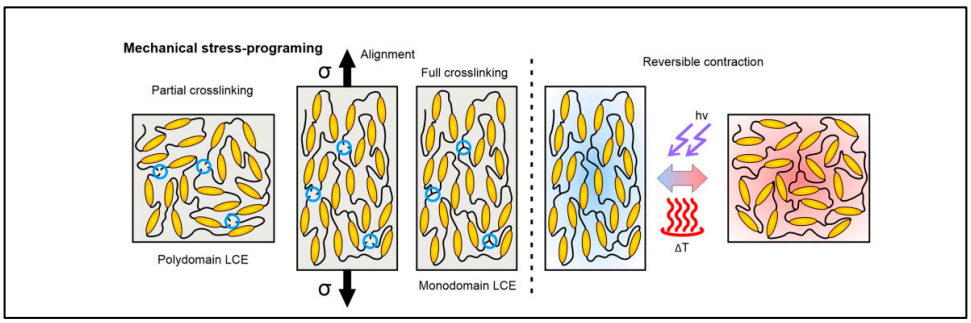


Figure 5. Schematic of the shape programming method for LCE [22].

Monodomain alignment of mesogens is achieved through several distinct strategies, depending on the level of control over complexity and the final output scale. Planar, 2D formats are conventional formats, and the material synthesis process puts constraints on alignment techniques due to the shape and size [22].

Mechanical alignment is one of the most frequently performed methods. In this method, a cross-linked LCE gel is deformed by stretching, bending, or twisting it to orient the mesogens along the stress axis, and a final crosslinking step fixes the alignment.

Effective for uniaxially aligned samples in bulk volume and capable of substantial linear actuation, it is challenging to precisely modulate the mesogen alignment over the material's volume or create complex, spatially varied director profiles [7]. More sophisticated geometries can be achieved by applying non-homogeneous stress fields, for instance, compressing LCE sheets against a mold [38].

Surface-enforced alignment as shown in Figure 6, is suitable for preparing thin LCE sheets with intricate, high-resolution mesogen patterns. LCE precursors are confined within an "alignment cell" composed of substrates coated with a command layer (e.g., rubbed polyimide or photoalignment materials), which indicates the mesogen orientation. In situ polymerization locks this surface-induced order, and the propagation of this order occurs through the materials. Surface-enforced alignment allows high-resolution patterning of director profile, which can be complex and can vary through thickness, but dimension is limited to thin films (up to several hundred micrometers), and can be a time-intensive process requiring specialized equipment [7,39].

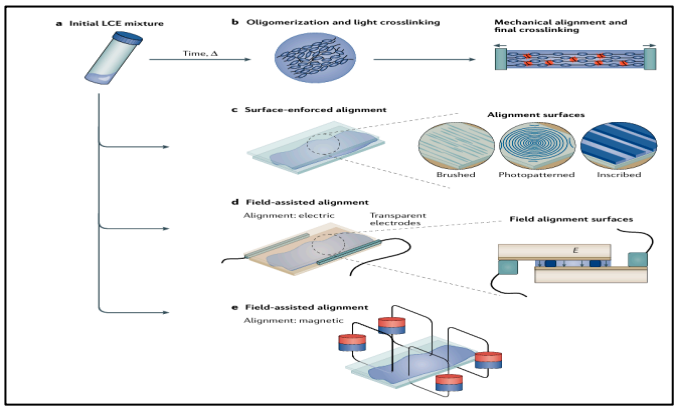


Figure 6. Alignment of LCEs by mechanical, surface-enforced, magnetic, and field-assisted methods. Reproduced with permission from Springer Nature [7].

Field-assisted alignment applies external electric (E-field) or magnetic (B-field) fields for mesogen orientation by leveraging their dielectric or diamagnetic anisotropy [7]. Before polymerization, low-viscosity LCE precursors are aligned by the field. While E-fields are limited to thin samples (up to 100 μm) due to the requirement of high field strength, B-fields can align larger and thicker specimens, making this a viable option for producing substantial monodomain LCEs [40]. The primary advantage of this non-intrusive method is its potential for integration with additive manufacturing to achieve complete 3D control over mesogen orientation, although up-scaled manufacturing remains a challenge [41,42].

Finally, rheological (shear-flow) alignment utilizes the shear and extensional forces generated during material extrusion to orient mesogens, obtained by DIW printing. While using DIW, as a viscoelastic LCE ink is extruded through a nozzle, the flow aligns the mesogens along the printing path. This alignment is immediately fixed by in situ curing. This approach uniquely enables the simultaneous programming of mesogen alignment and 3D geometry, allowing for the fabrication of intricate structures with locally controlled director profiles [31]. While this technique has gained popularity for its versatility, mesogen alignment is currently achievable only within the parallel plane of deposition, necessitating advanced printing strategies to achieve out-of-plane actuations [22].

3. Additive Manufacturing Mechanisms of LCE

Additive manufacturing brought a revolution for the manufacturing of diversified materials in the past decades, creating customized production for a specific scope. With

the help of 3D printing techniques, the LCEs could not only be manufactured in desired 3D structures but also they can have director fields that are controllable. The actuated shape morphing obtained by 2D transitions to 3D transitions by applying external stimuli could also be precisely controlled. The printing techniques of the LCE have gained much attention and are regarded as one of the most important breakthroughs in diverse fields of research [43]. To achieve the actuation performance that is desirable, both the director fields and the shapes of the LCEs are required to be precisely controlled. Thus, the alignment of mesogens should be incorporated into the 3D printing processes, which often adds new challenges. Based on the solidification process, 3D printing of polymeric materials can be classified into the following categories: materials extrusion, vat photopolymerization, powder bed fusion, material jetting, etc. [44].

Unlike LCEs produced through traditional fabrication techniques, 4D-printed LCEs can be manufactured with intricate geometries, diverse functionalities, and tunable sizes ranging from the microscale to the macroscale. Additionally, they enable the seamless integration of various active and passive materials. As a result, 4D-printed LCEs exhibit more sophisticated pre-programmed actuation modes and higher actuation energy output, supporting applications that span from centimeter-scale energy-dissipating devices to sub-micrometer micro actuators [45]. In this section, different major additive manufacturing processes are discussed. Their unique features, complexity of implementation, and how they are advancing the LCE manufacturing process are highlighted.

3.1. Direct Ink Writing (DIW)

Among the available material extrusion-based additive manufacturing methods, direct ink writing (DIW) is a preferred candidate for manufacturing LCEs. DIW uses viscoelastic, shear-thinning inks that flow under pressure but, after deposition, rapidly recover to retain their shape. This unique property of the inks makes DIW the only feasible extrusion-based approach for printing LCEs. Since curing can fix both the 3D geometry and molecular alignment, the fabrication of LCEs with programmable stimuli-responsive behavior and complex centimeter-scale geometries is possible [31–33]. DIW-printed LCEs can deliver amplified actuation strains and diverse property changes under external stimuli than the thin films produced by FFF or other methods, making them highly attractive for diversified applications [45].

In a DIW setup, as shown in Figure 7a, the ink is extruded through a nozzle and deposited layer by layer along predetermined paths to build up a 3D structure [46]. The viscoelastic LCE inks are formulated to display shear-thinning for smooth extrusion and rapid recovery for shape retention. To prevent collapse or deformation, rapid solidification is essential. Thus, DIW printers are often equipped with auxiliary devices such as heaters (to accelerate solvent evaporation) or UV lamps (for in situ curing). Inside the nozzle, the shear and elongational stresses promote mesogen alignment, an effect that has been widely observed in other processing methods such as electrospinning and fiber drawing [47,48]. This alignment mechanism is particularly advantageous for LCEs, as it couples material flow with director orientation during printing.

A DIW printer used, in general, for LCEs includes an XYZ direction motion-controlled platform, an extrusion nozzle, and a photocuring setup. A heater is added around the ink barrel to reduce viscosity without altering solidification kinetics for some specific applications [31]. During printing, extruded filaments are deposited line by line with controlled X–Y movements, while simultaneous UV curing locks in the shear-induced alignment at each step.

The printing parameters also have a vital role in determining mesogen alignment and actuation. By precisely tuning ink composition, process conditions, and toolpath

design, DIW enables the creation of highly versatile LCE architectures with complex, programmable actuation behaviors. The printing temperature has a strong influence on viscosity and director ordering. Higher temperatures provide better extrusion, but they would also weaken alignment. In the mesophase stage (10–20 °C below T_{NI}), printing yields higher-order parameters and larger actuation strains [49]. Printing speed can also locally tune molecular alignment and contraction strain, ranging from 0.5 to 28 mm s^{-1} [5,50]. Nozzle diameter further affects resolution and alignment. Smaller diameters (150–1400 μm) yield stronger orientation, but it would require higher pressures [5,51,52]. Above all, the programmed printing path dictates the functional actuation response: uniaxial paths result in in-plane contraction, whereas orthogonal paths induce bending or twisting, and +1 azimuthal patterns generate conical deformations [53].

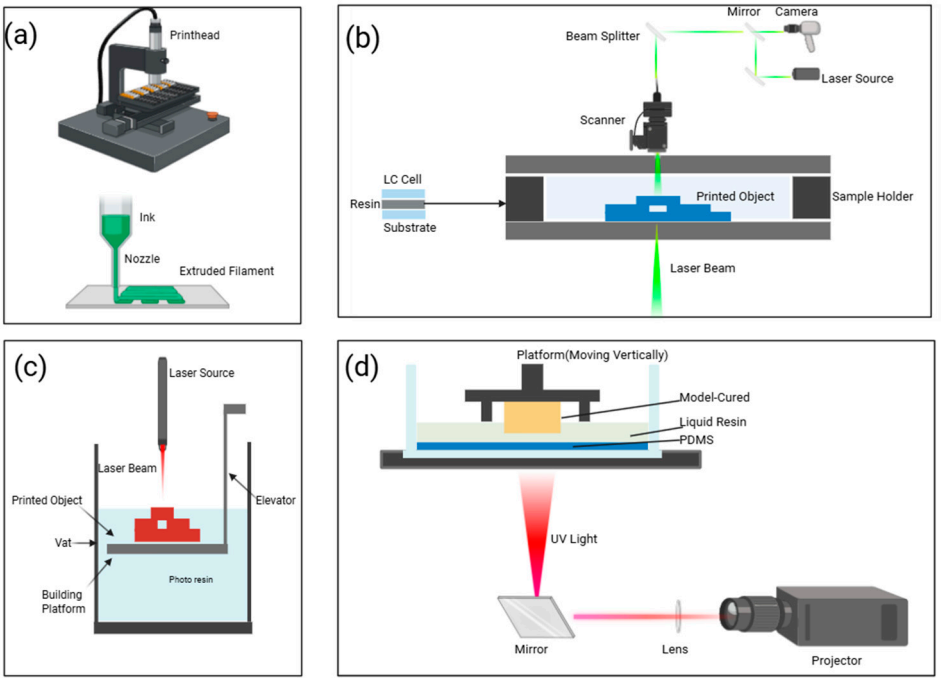


Figure 7. Schematic diagrams of (**a**) DIW printing; (**b**) DLW-TPP system; (**c**) VP system; (**d**) DLP system.

3.2. Vat Photopolymerization (VP)

The growing demand for miniaturized and high-resolution LCE-based devices has driven extensive research into their integration in diversified fields spanning micro photonics, microfluidics, and micro robotics [48,54,55]. For manufacturing such applications, fabrication methods with the ability to generate precise microscale features are required. Vat photopolymerization (VP) has been considered as a promising approach, offering well-established capabilities for constructing three-dimensional objects with micrometer and even sub-micrometer resolution [56–58]. This high spatial accuracy allows the direct fabrication of functional LCEs with complex geometries and arbitrary architectures, positioning VP as a key method for translating LCEs into next-generation microdevices.

VP utilizes light irradiation for selective polymerization of resins in a layer-by-layer manner, as shown in Figure 7c [59]. In this process, the inks are composed of polymerizable mesogens with low viscosity in the LC state. Before curing, these mesogens are aligned by external fields such as surface templates, electric fields, or magnetic field [60]. Once alignment is established, photopolymerization is triggered within selected regions, shaping the 3D structure while fixing mesogen orientation layer by layer. Through this approach,

director fields can be precisely tuned by modifying the design of the surface template or adjusting the applied external field.

Two VP printing strategies are commonly employed: the first one is two-photon polymerization (TPP). It is a direct laser writing process in which a focused laser beam scans through the resin to define aligned thin layers [61]. TPP provides the highest resolution among all LCE printing techniques, which is less than 200 nm, and uniquely enables the continuous alignment of mesogens along the *z*-axis, a feature not achievable by extrusion-based printing methods like DIW. However, the alignment thickness of the liquid crystal layer is typically limited to approximately 100 μm, which imposes a constraint on the maximum size of printed structures. The second one is digital light processing (DLP), which constructs 3D shapes by exposing each layer to a patterned light field [62–64]. In this method, substrate movement during layer-by-layer printing can disrupt mesogen alignment, thus making it necessary to restore order by applying magnetic fields or shear forces. Furthermore, when different alignment patterns are required across successive layers, the printing time may increase rapidly.

3.2.1. Two-Photon Polymerization (TPP)

Direct laser writing process based on Two-Photon Polymerization (DLW-TPP) has emerged as one of the most precise additive manufacturing (AM) strategies, achieving spatial resolutions down to around 40 nm, which is significantly beyond the reach of most conventional AM methods [13]. For photonic and soft matter applications, the ability to construct free-form three-dimensional (3D) architectures with sub-micrometer accuracy has made DLW-TPP a perfect candidate. For LCE manufacturing, this resolution is advantageous because nanoscale or microscale surface morphologies provide strong anchoring energies to dictate mesogen orientation. As a result, DLW-TPP has been widely utilized to create 2D or 3D structures with spatially defined molecular alignment, and it is applied in adaptive microlenses, tunable displays, and other reconfigurable optical elements [65–68]. The first demonstration of DLW-TPP applied to LCEs was reported by Sungur et al., where thermally responsive gratings with features below the diffraction limit, close to 50 μm were fabricated, exhibiting reversible step contractions of up to 20% under heating and cooling cycles [69].Their research demonstrated the potential of DLW-TPP in coupling nanoscale structural fidelity with stimuli-responsive polymer systems.

In general, the DLW-TPP system, illustrated in Figure 7b, employs a top-down configuration consisting of a femtosecond laser source, optical scanning and focusing components, a resin vat, and a platform [13,58]. To facilitate the mesogen alignment, the vat is often replaced with an LC cell containing micropatterned or conductive substrates. During printing, ultrashort laser pulses are focused into the resin, where simultaneous absorption of two photons triggers localized polymerization on a voxel-by-voxel basis(Figure 7b). Followed by laser writing, the unreacted resin is removed through development, which leaves behind a highly resolved polymer network. Here, the resolution is defined not by the optical diffraction constraint but by the laser focal volume.

The inks used for DLW-TPP consist of three elements: a two-photon photoinitiator, monofunctional RMs or isotropic cross-linkers, which can adjust cross-link density and bifunctional reactive mesogens (RMs) to establish the network [58] Acrylate-based RMs remain the most common option, but their oxygen sensitivity has prompted exploration of epoxide and oxetane RMs, which use photo-cationic polymerization [70]. In addition, to impart light-driven or thermal responsiveness, functional dopants such as azobenzene chromophores or photothermal nanoparticles have been incorporated when their absorption profile permits efficient two-photon activation at 720–780 nm with polymerization at 390 nm [58].

The performance of DLW-TPP-printed LCEs is dependent on processing parameters like writing speed, energy, and temperature, which govern the polymerization degree, cross-link density, and mesogen alignment. For instance, higher energy or slower writing improves conversion but reduces actuation strain, while lower writing temperatures can suppress resin swelling and improve printing resolution. Conversely, higher temperatures would decrease resin viscosity but compromise orientational order. Combining DLW-TPP with patterned substrates or electric-field alignment can ensure additional control, enabling precisely tuned mesogen orientation and programmable actuation [13]. These advantages make DLW-TPP a suitable method of manufacturing complex 3D LCE architectures with tailored anisotropy and microphotonic features. Compared to other methods, such as direct ink writing (DIW) or stereolithography (SLA), DLW-TPP remains unmatched in terms of spatial resolution and control over molecular orientation. However, its relatively slow build rates and high equipment costs limit the scalability. While DIW is better suited for larger structures, SLA provides higher throughput; neither technique, however, offers the nanoscale structural precision essential for photonic and biomedical LCE applications. Thus, DLW-TPP stands out as a critical enabling tool for advancing the design of next-generation LCE actuators and functional devices.

3.2.2. Digital Light Processing (DLP)

DLP has emerged as an advanced procedure for the fabrication of LCEs, which employs a digital micromirror device (DMD)-based projector for selective trigger photopolymerization of resins in a layer-by-layer manner [63]. However, additional reorientation steps are essential because the required vertical lifting of the substrate after each layer could disrupt mesogen alignment. To overcome this challenge, Tabrizi et al. integrated a rotatable magnetic field (300 mT) into the DLP process, which enabled two things: Firstly, voxel-by-voxel alignment (Figure 7d) and secondly, allowed complex 3D mesogen patterns to be programmed within each layer [41]. While this approach extended design flexibility, the long dwell period, which is around 5 min per voxel constrained speed. Li et al. resolved these issues by introducing a shear-flow alignment mechanism that performed mesogen orientation before photopolymerization, and it reduced the entire printing cycle below 10 s per layer and printing speed in 120 μm/min in z-direction, enabling faster fabrication of actuators that are capable of reversible grasping, crawling, and weightlifting [71].

Compared with polydomain structures, DLP-printed monodomain LCEs are preferred because of their anisotropic mechanical response and large actuation strain. Li et al. achieved this by using cyclic resin tray rotation to generate shear forces, fabricating actuators with programmable gripping, crawling, and lifting functions. These devices delivered a specific work capacity of 63 J kg^{-1} and thermally induced strain of 50%, both exceeding human muscle performance, which are 40 J kg^{-1} and 20% [71].

Further advances by Chen et al. introduced reprogrammable dual-phase LCE networks with a crystalline melting transition (90 °C) above the mesophase transition (58 °C), allowing reversible locking and unlocking of alignment and enabling diverse, reconfigurable 3D thermal-responsive actuators [72]. These results underline DLP's potential to integrate high resolution, programmable alignment, and multifunctionality into LCE devices.

In comparison with other existing methods, DLP holds a middle ground between DIW and TPP. DIW offers the fastest printing speed and scalability with shear induced alignment but it is often limited in resolution and primarily suited for actuators with thicker dimension approximately in centimeters scale [41]. On the contrary, TPP process ensures the finest resolution (200 nm) and continuous 3D alignment but printing speed is very slow and constrained to small volumes [62]. DLP therefore provides a balance: it offers higher

resolution (50 μm) and more precise 3D alignment than DIW, while being faster and more scalable than TPP [41,71].

4. Application of LCE-Based Actuators in Soft Robotics

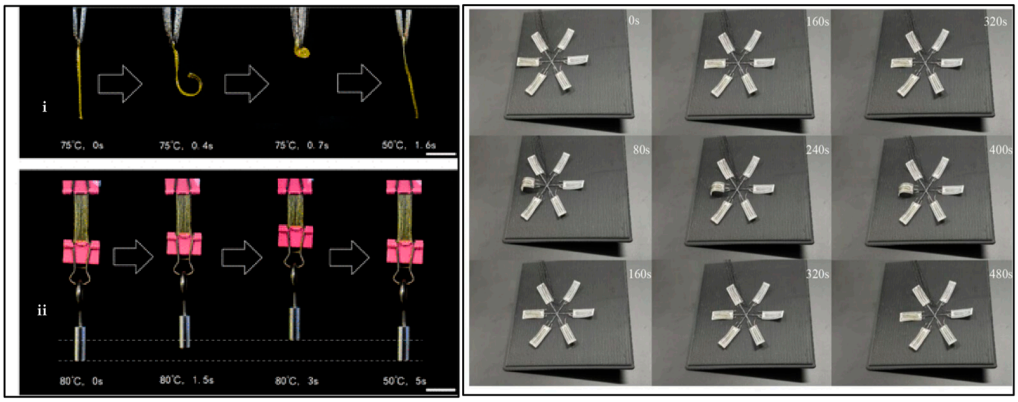
Additive manufacturing transformed liquid crystal elastomers (LCEs) from thin-film demonstrations into programmable three-dimensional actuators. Using DIW, shear alignment during extrusion and ultraviolet curing locked mesogen orientation directly into the printed structure, which eliminated the need for mechanical pre-alignment. This approach by Ambulo et al. enabled anisotropy to be defined by the print path itself, producing filaments with 40% reversible contraction, twisted bilayers, lattices that collapsed volumetrically, and defect-encoded sheets that morphed into cones. The design of shells combining positive and negative Gaussian curvature underwent snap-through instabilities: rapid inversion within 16 ms, momentary airborne motion for 64 ms, and recovery on cooling. These actuators not only supported loads which were several times their mass but also reached specific powers around 15.5 W kg^{-1}, which demonstrated that coupling programmed alignment with geometry could produce high-speed, high-power, and reversible actuation suitable for soft robotics [32].

As proof of rapid actuation established its potential, López-Valdeolivas et al. focused on achieving thicker, load-bearing LCE bodies through DIW combined with in situ photopolymerization. By maintaining alignment during extrusion and crosslinking, robust free-standing structures were manufactured, which surpassed the limitations of thin-film dimensions. Single filaments contracted by 50%, and lightweight multilayer stripes with a mass of around 0.17 g lifted weights of up to 20 g, corresponding to a specific work of around 1.44 J kg^{-1}. Orientation control was extended spatially, producing spirals that curled into cones, slit arrays, auxetic honeycombs with tunable pore shapes, and chiral frames with rotational capability. Their work also introduced functional integration by embedding a printed LCE ring into polydimethylsiloxane (PDMS) to create a variable-focus lens with thermally tunable curvature. Such advances highlighted not just structural scaling but also multifunctionality, bridging material actuation with device-level applications in optics and haptics [33].

Hybrid fabrication strategies merged printing with assembly to integrate electrical control directly into LCE systems. By combining DIW of conductive silver wires, and pick-and-place assembly of pre-aligned LCE strips, Yuan et al. produced laminated hinges that bent more than 150° when Joule-heated above 87 °C, then recovered on cooling. These hinges acted as modular building blocks for active architectures, enabling demonstrations like a morphing airplane, a miura-ori sheet, a sequentially folding box with addressable heating, and a crawler that would advance 10% body length per cycle. This hybrid method demonstrated that LCE actuators can be integrated into deployable and reconfigurable robotic systems by combining printed electronics with responsive strips. Unlike the previous works focusing on high-speed instabilities [32] or emphasis on scalable thickness and multifunctionality [33]. Their work provided that electronics and thermal actuation could be integrated into modular assemblies, pointing directly toward robotics and deployable devices [73].

Taken together, these efforts established three critical directions: direct encoding of alignment for fast and powerful response [32], structural scaling for load-bearing and multifunctional use [33], and hybrid integration of heaters and actuators for programmable, system-level function [73]. These complementary advances formed the technological basis for the subsequent expansion of LCE printing into gradient design, property grading, multimodal actuation, and functional feedback.

Zhang et al. achieved the ability to design orientation gradients within printed LCEs. They accomplished this by extruding a single-component LCE ink in the isotropic state at 200 °C onto a cryogenic stage held at 10 °C (Figure 8a). Cooling during the deposition process could induce nematic alignment while the nozzle's drawing force generated gradients across the filament thickness. Photodimerization provided stability, and then these gradients enabled bending coupled with contraction rather than uniaxial stroke. Printed strips curled into hollow cylinders with radii near 1 mm, recovered upon cooling, whereas lightweight double-layer strips (0.02 g) lifted 12.56 g, which was about 600 times their mass. Porous sheets transformed into cylinders within 0.1 s and relaxed within 1.75 s, and hybrid structures demonstrated "9-type" and "B-type" multimodal actuation. These findings indicated that orientation could be designed as a field variable, expanding LCE actuation beyond contraction into programmable morphing [5].



(**a**) (**b**)

Figure 8. (**a**): (**i**) Photograph of reversible bending deformation process of a printed strip upon heating and cooling. During heating and cooling processes between 50 and 75 °C, bending−extension deformation behavior was observed. Scale bar: 4 mm. (**ii**) Photograph of weight-lifting of a printed double-layer strip (0.02 g). A weight of 12.56 g attached to the strip can be lifted up for 7 mm reversibly upon heating and cooling. Scale bar: 10 mm. Reprinted with permission from [5]. 2019, American Chemical Society. (**b**) Multilegged controllable deformation soft robot: Physical image of the soft robot moving on a 20° inclined plane in single-foot actuation mode [74].

The idea of printing properties as fields was extended by Wang et al., by fabricating functionally graded LCEs using DIW printing. By tuning the printing temperature, nozzle gap, and nozzle size, they controlled the balance between aligned shells and polydomain cores in each filament. This directly mapped process to performance: strains up to 61% and stresses near 300 kPa were obtained under optimized conditions. Functionally graded disks were warped into distinct 3D shapes, bilayer petals were bent and twisted in programmed ways, and auxetic lattices exhibited switchable Poisson's ratios. Graded LCE tubes bonded to rigid glass mitigated stress and avoided delamination that plagued homogeneous constructs. Their contribution showed how manufacturing parameters could be connected not only to prescribe motion but also to design durability and load-bearing capacity into LCE systems [49].

Apart from DIW, digital light processing (DLP) also advanced the manufacturing process with higher precision and new functions. Luo et al. employed a photocurable LCE resin to print periodic foams with porosities of 62–85%. Unlike conventional foams, they dissipated energy not only through viscoelasticity but also through mesogen rotation, yielding 1.8 to 4.8 times greater energy absorption than non-LCE foams at room temperature

and up to 81% at 40 °C. Stretching-dominated lattices (Z = 12) were especially efficient, and the foams protected fragile objects such as eggs during drop tests. This reframed LCEs as impact-mitigating and protective materials, expanding their role beyond actuation into energy dissipation and cushioning [75].

Self-sensing was introduced to make LCE actuators more autonomous. One approach exploited the phase-dependent optical transition of LCEs, where opacity in the nematic state and transparency in the isotropic state provided a built-in strain signal. This enabled actuators with high work output that could bend, grasp, crawl, and lift loads over 700 times their mass, combining versatility with exceptional strength [71]. A complementary strategy used by Kotikian et al. implemented a core–shell direct ink writing method to print coaxial fibers with liquid-metal cores encased in aligned LCE shells. These innervated structures combined heating and resistance-based sensing in the same body, producing contractions of nearly 50%, lifting more than 200 times their weight, and enabling closed-loop control of programmed deformations [76]. Together, these optical and electrical pathways showed how sensing could be seamlessly integrated into LCE actuators to achieve regulation in real-time level.

Together, these contributions demonstrate how printing progressed from defining orientation to programming gradients, grading mechanical properties, and adding new functions such as energy dissipation and intrinsic sensing. Orientation gradients expanded the actuation repertoire) [5]; functional grading linked process with durability and load handling [49]; foams reframed LCEs as protective materials [75]; and self-sensing actuators integrated feedback with actuation [71]. These initiatives influenced LCE printing toward multifunctional, feedback-enabled systems suitable for robotics, biomedical devices, and adaptive structures.

Song et al. demonstrated that optimization of direct ink writing (DIW) parameters could directly influence actuator performance and robotic locomotion. By controlling nozzle size, extrusion pressure, and temperature, they fabricated filaments that exhibited approximately 42% strain, stresses of 0.33 MPa, and contraction times as short as 2.5 s. Integrated with PDMS feet patterned with tilted scales for anisotropic friction, these actuators powered an inchworm-inspired crawler that moved at 4.3 mm per minute, showing how fine process control at the filament scale could be translated into efficient system-level performance [77]. Wang et al. extended this concept toward photothermal actuation by developing a 3D-printable LCE composite ink with only 0.1 wt.% gold nanorods, as shown in Figure 9. This low filler loading delivered a photothermal response of 27% strain without compromising mechanical properties, which was a key improvement over earlier composites. Using DIW, they printed a fully untethered, light-driven walker that was significantly larger and heavier than prior works. Yet, it was capable of stable locomotion on inclined and complex surfaces. Locomotion speeds up to 0.284 mm s^{-1} were achieved by adjusting ratchet surface design and localized light exposure, demonstrating scalable and controllable light-responsive actuation [78]. While both approaches optimized single-mode actuation, Peng et al. introduced polymerization sequence control in double-network LCE–polyurethane composites. Depending on the sequence, actuators displayed either cooling-induced elongation by 61% or contraction by 15%. Combining these responses, multimodal behaviors were displayed, such as twisting, kirigami folding, and tug-of-war actuation. Complex morphing structures including lanterns, towers, and octopuses fabricated via DLP further highlighted the shift from unidirectional actuators to programmable, multimodal systems [79].

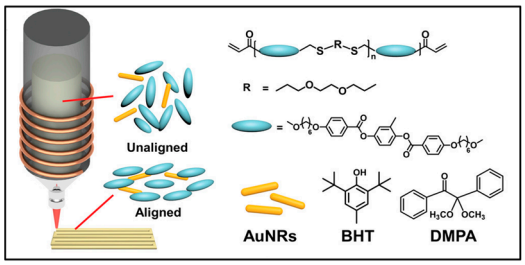


Figure 9. Schematic illustrations of the DIW printing of the AuNR/LCE ink: the molecular structures of the AuNR/LCE ink. Reproduced with permission from [78].

Vinciguerra et al. focused on electrical integration and developed a multimaterial DIW method to co-print LCEs with conductive composites of gallium–indium alloy, silver flakes, and elastomer. The printed pathways functioned as both Joule heaters and interconnects, enabling actuators that powered LEDs, transmitted Morse code through twisting, and incorporated capacitive sensing within the same body [80]. In parallel, Sgotti Veiga et al. improved practical applications with UV-assisted DIW, introducing biphasic liquid-metal conductors and dual-sided curing reduced polymerization time to approximately 90 s. Their actuators achieved bending angles of 320° under only 2.5 V while consuming 620 mW cm^{-2}, combining low-voltage operation with strong durability across repeated cycles [81]. Together, these studies marked the transition of LCEs from thermally activated devices to fully printed, electrically integrated actuators.

Kotikian et al. further extended programmability by creating multimaterial lattices composed of LCE inks with distinct nematic–isotropic transition temperatures of 65 °C and 125 °C. In triangular lattice architectures, low-transition struts actuated first, followed by high-transition struts, yielding sequential pathways such as shear morphing or hourglass contraction. Supported by an inverse-design framework coupling thermoelastic modeling with optimization, this approach applied predictive control of bilayer bending and star-like morphing, demonstrating multistage actuation as a design paradigm [82].

Reinforcement strategies addressed mechanical fragility by adding new functionality. Jiang et al. developed a DIW platform that infused continuous fibers into LCE resin, where during extrusion, shear flow aligned mesogens. The selection of fiber tailored performance was due to the reasons that carbon fibers improved stiffness, polyester fibers enhanced flexibility, and conductive fibers enabled Joule heating. These composites produced grippers, spirals, and flower-like actuators with energy absorption level nine to fifteen times higher than pure LCEs [83]. Zhang et al. expanded on this approach by co-printing continuous carbon fibers that both reinforced structures and acted as electrothermal heaters. Their actuators recorded response time of 20 s, bending curvatures of 0.25 mm^{-1}, and drove robots capable of climbing 20° inclines and lifting objects twenty times their own weight (Figure 8b). Together, these works overcame fragility while coupling reinforcement with heating to enable robust, multifunctional actuation [74].

Building on these advances, Xia et al. developed untethered machines by integrating reinforcement, low-voltage heating, and electronics. Silicone-encapsulated LCE actuators with embedded polyimide heaters were tuned to lower transition temperatures to approximately 40 °C, allowing operation at 3.7 V. These actuators bent 162° within 30 s, remained stable over 50 cycles, and powered a 9.87 g robot that crawled at 0.28 body lengths per minute, lifted 1.5 times its weight, and traversed obstacles with a cost of transport of 7: demonstrating the most efficient electrically driven LCE robot reported to date [84]. Yuan et al. complemented this direction by integrating liquid metals to realize multimodal locomotion. DIW sandwich actuators, embedding an EGaIn–alginate electrothermal layer between active and passive LCE layers, achieved bending angles of 270° under 1.5 V and

switched between crawling and flipping behaviors depending on the input voltage. An X-shaped robot crawled at 6.1 mm/min and flipped robustly under higher voltages, illustrating how multimodal motion can be integrated into a single actuator architecture [85].

Herman et al. worked on solving the long-standing challenge of molecular alignment in the VP process by combining a low-strength magnetic field of 100 mT with DLP printing. This enabled complex free-form geometries with voxelated, through-thickness orientation control. By programming layer-by-layer alignment, they fabricated LCE objects with pre-programmed instabilities and complex actuation modes, providing a pathway for architected devices with high spatial fidelity and functional complexity [86].

5. Applications in Biomedical Technology

The integration of LCEs with 4D printing has extended new horizons in biomedical engineering by enabling the design of adaptive, stimuli-responsive, and dynamic devices. Unlike conventional biomaterials, LCEs integrate molecular anisotropy with elastomeric elasticity, which allows large, reversible shape transformations under stimuli such as heat, light, or mechanical fields. When paired with additive manufacturing, these unique characteristics translate into programmable objects tailored to patient-specific needs, ranging from minimally invasive implants to wearable systems. This section highlights key advances, organized into thematic categories ranging from Bioprinting, Implantable Devices, to Wearables and Artificial Muscles, to provide a structured overview of the diverse biomedical directions enabled by LCE-based 4D printing.

5.1. Bioprinting

Bioprinting has become a cornerstone in tissue engineering and regenerative medicine, offering automated, layer-by-layer deposition of bioinks with high spatial resolution, scalability, and reproducibility. Bioinks typically comprise hydrogels, which are derived from natural, synthetic, or hybrid biomaterials: encapsulating cells that are stabilized by cross-linking during or after printing [87]. While conventional bioprinting techniques allow the creation of complex architectures, reproducibility and versatility remain critical challenges. To address these, biofabrication has been redefined as the automated creation of biologically functional products from biomaterials, living cells, and bioactive molecules, employing strategies such as bioprinting and post-print tissue maturation [88]. Within this framework, 3D bioprinting stands out for its capacity to synchronize material deposition and cross-linking, enabling programmable constructs [88–90] Furthermore, the incorporation of synthetic bioinks has advanced cellular responses, biocompatibility, and extracellular matrix (ECM) formation, thereby widening the biomedical potential of printed scaffolds [88,91].

Expanding this foundation, Saed et al. pioneered the application of LC-based inks for 4D printing [92]. Their thiol-acrylate/thiol-ene “click” chemistry helped to develop LCE-based materials with tunable thermomechanical properties, capable of exhibiting sequential, reversible, and multishape transformations across a wide thermal range. This work underscored the adaptability of LC-based 4D printing in generating morphing scaffolds and smart biomedical devices. Davidson et al. advanced this concept by developing reconfigurable LCEs that employed light-triggered dynamic covalent bond exchange [93]. Their DIW-based process integrated chemistry and printing to achieve reversible actuation, permanent shape locking, and multimaterial constructs with region-specific actuation. Together, these contributions highlight bioprinting as not just a tool for static architectures but as a platform for adaptive scaffolds and intelligent biomedical devices capable of dynamic interaction with their environment.

5.2. Implantable Devices

The transformative potential of LCEs for implants was exemplified by Volpe et al., who fabricated 3D-printed semi-crystalline LCE spinal fusion cages [94]. These devices utilized the unique phase transitions of LCEs: soft and amorphous during insertion for minimally invasive implantation, yet crystallizing afterward to provide mechanical stiffness for load bearing. Notably, the modulus increased from 8 to 80 MPa post-implantation, and the constructs endured over one million compressive cycles with minimal creep. This dual-state performance addressed limitations of traditional spinal cages, which often failed due to rigidity, poor fit, or subsidence. The ability to print patient-specific geometries represented a significant step toward customized implants.

When contextualized alongside earlier works, such as LC-based 4D printing for shape-morphing scaffolds and smart biomedical devices [92] and developing reconfigurable LCEs with light-triggered dynamic covalent bond exchange [93]. Volpe et al.'s study illustrated how LCE functionality can move from proof-of-concept morphing systems to clinically relevant devices [94]. The paradigm of phase-dependent mechanics directly supports the goal of minimally invasive yet stable orthopedic implants, highlighting how 4D-printed LCEs may redefine implant design across other load-bearing tissues as well.

5.3. Bioresponsive and Living Systems

Beyond structural implants, 4D-printed LCEs have also been applied to engineered living materials (ELMs): composites that combine living cells with synthetic matrices to achieve programmable responsiveness. While early ELMs, which were produced by molding, lacked spatial resolution [88,95], the advent of 3D and 4D printing has enabled precise spatial control over microbial distribution and bio-responsive functionality [96]. Rivera-Tarazona et al. demonstrated this concept by formulating inks with cellulose nanocrystals (CNC) to control rheology and facilitate multimaterial printing of yeast strains, as shown in Figure 10 [95]. They fabricated capsules that ruptured upon amino acid exposure, releasing encapsulated payloads, thereby providing proof-of-concept for drug delivery systems [95,97].

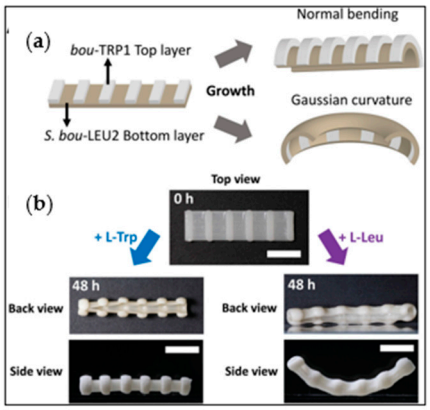


Figure 10. D printing ELMs capable of multiple shape change: (**a**) Schematic of a printed bilayer composed of two engineered *S. boulardii* mutants. The top layer is printed as stripes, and the bottom layer as a flat sheet. (**b**) Printed structure is able to shape into two different types of geometry. When the bilayer is incubated in synthetic medium lacking L-leucine, it changes shape into a tube-like structure (left). When being incubated in synthetic medium lacking L-tryptophan, the bilayer adopts a geometry with two types of bending (right) (Scale bars: 10 mm) mode. Reproduced with permission from [95].

Advances in LCE fabrication are aligned with these bioresponsive systems. McDougall et al. worked on embedded printing, where LCE inks were extruded within

removable gelatinous supports, producing UV-cured freeform structures that exhibited reversible shape morphing without requiring external supports [10]. Similarly, Dai et al. introduced the concept of how DIW could produce both monodomain and polydomain nematic LCEs with distinct shape-memory effects [98]. Their bilayer structures exhibited one-way and two-way shape-memory cycles, which enabled non-monotonic recovery paths. This highlights how control over alignment and domain structure can generate adaptive shapes, though intrinsic softness continues to limit high-rigidity applications. These works emphasized that bio-responsive systems, whether incorporating living cells or relying on intrinsic material dynamics, benefit from 4D-printed LCEs as enabling platforms for adaptability and responsiveness in biomedical contexts.

5.4. Wearables and Artificial Muscles

Wearable biomedical devices and artificial muscles represent another domain where LCE-based 4D printing is making a profound impact. Li et al. introduced a hybrid cooling-assisted DIW process to overcome constraints in near-ambient temperature-responsive LCEs (NAT-LCEs) [99]. By integrating a liquid-cooled nozzle and a cold substrate, they improved mesogen alignment by nearly 3000% compared to standard DIW, yielding printed sheets with superior order and reproducibility. These NAT-LCEs underwent bidirectional deformation under heating and cooling, and their proof-of-concept wristband could adjust tightness dynamically to improve heart-rate monitoring accuracy. This demonstrated how careful process innovation can directly translate into biomedical wearables with adaptive functionality.

With inspiration from natural thermoregulation, He et al. designed LCE-based skin actuators that mimic sweat glands [100]. Printed DIW filaments achieved strains of 40.4%, with chamber actuators capable of discharging water during actuation. When arranged in arrays, these actuators delayed temperature rise and stabilized local environments, achieving a 10 °C reduction compared to controls. This biomimetic approach underscores the potential of LCEs in autonomous thermal management and wearable biomedical devices.

To complement these planar systems, Hou et al. reported a liquid crystalline spinning process inspired by spider silk, producing continuous and highly aligned LCE microfibers at remarkable speeds (8400 m h^{-1}) [101]. The resulting fibers lifted 2000 times their weight, generated stresses up to 5.3 MPa, and operated at 50 Hz, significantly exceeding the performance of existing artificial muscles. Its applications span from prosthetic limbs to robotic surgical tools. In parallel, Roach et al. developed a roll-to-roll DIW process for nano clay-modified LCE fibers that were mechanically robust and long enough (up to 1.5 m) for integration into textiles [102]. These smart fibers exhibited reversible actuation strains of 51% and could be incorporated into clothing with thermoresponsive pores, demonstrating applications in wearable medical textiles and biosensing garments.

Taken together, these studies demonstrated how wearables and artificial muscles leveraged both the fine control of DIW and the scalability of fiber spinning to produce robust, adaptive, and multifunctional biomedical systems.

5.5. Programmable and Light-Responsive Actuators

The pursuit of programmable, stimuli-responsive actuators has also been advanced by 4D-printed LCEs. Sol et al. introduced high-temperature DIW of a single azobenzene-functionalized cholesteric oligomer ink (Figure 11) [103]. By tuning the nozzle speed and photopolymerization delay, they created three distinct mesophase domains, each with unique optical and bending responses, within a single print job. This enabled multimodal actuation using only a single material, simplifying fabrication while expanding design possibilities.

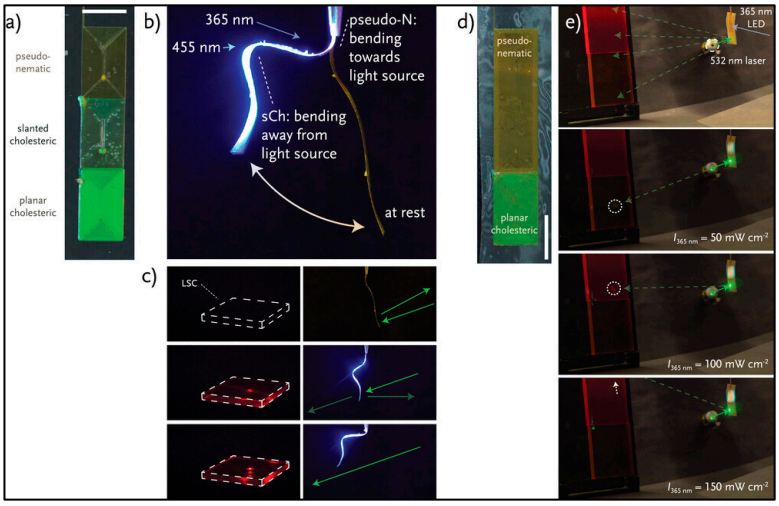


Figure 11. (**a**) Photograph of the multimesophase film printed on PEI foil where the locations of the uniaxial pseudo-nematic, slanted cholesteric, and planar cholesteric domains were indicated. (**b**) Combined photographs highlighting complex actuation behaviors using the different mesophase domains. λ = 365 nm and λ = 455 nm wavelength lights were used to irradiate the film simultaneously. (**c**) Illustrative comparison showing how the reflective element on the actuator could be used to intercept, wholly or partially, a λ = 532 nm laser beam, or leave it to pass untouched. The left column photographs demonstrated a luminescent device using fluorescent dye 7 acting as an optical sensor for the incident laser beam. The photographs in the right column served purely illustrative purposes. (**d**) Photograph of an alternative device design, a large uniaxially planar pseudo-nematic section for actuation or light steering, and a planar cholesteric section for light reflection. (**e**) Demonstration of irradiance-dependent light steering. A λ = 532 nm laser was directed towards the reader at the planar cholesteric section and obliquely reflected to a luminescent device at a distance. An λ = 365 nm LED (intensity indicated in each image) is applied to actuate the ChLCE films and redirect the incident laser light. Markers were added to indicate the laser path (dotted line), LED light direction (solid green line), and position of the reflected laser spot on the luminescent devices (dotted white circle: top fluorescent plate uses dye 7, bottom uses dye 8). NB: the scale bar in (**a**,**d**) corresponds to w = 6 mm [103].

In a complementary direction, Prévôt et al. employed photocrosslinkable smectic-A LCE inks with desktop DLP stereolithography, which replicated biological templates like mouse brain vasculature [104]. Their scaffolds not only preserved structural fidelity but also imparted intrinsic molecular alignment, guiding fibroblast growth along struts. This biomimetic printing strategy directly linked material alignment with cell organization, holding strong implications for tissue engineering and regenerative medicine.

These advances illustrate how programmable LCE constructs, whether through light-triggered phase control or bioinspired templating, expand the design space for biomedical actuators. Importantly, they demonstrate that optical, mechanical, and biological functionalities can be simultaneously encoded into printed geometries, a hallmark of multifunctional biomedical systems.

6. Challenges and Future Perspectives

6.1. Challenges

LCE fabrication is highly reliant on the synthesis of inks suited to the specific manufacturing process. For DIW, most inks depend on shear-thinning acrylate mesogens that can be oriented during, but only a limited set of commercially available diacrylate mesogens meet these requirements [4]. This also restricts the range of mechanical properties and actuation temperatures. Although epoxide-reactive mesogens reduce polymer shrinkage and oxygen sensitivity, such inks are still in their infancy [45]. Increasing cross-link density

suppresses swelling yet reduces actuation strain; incorporating reversible physical cross-links or dynamic covalent bonds may allow tunable network density and reprogrammable structures [105]. Multistimulus responsiveness via photothermal or electroactive dopants can lead to filler aggregation and phase separation [106]. These challenges make ink selection and design an essential part of the 4D printing process.

6.1.1. Challenges for the Printing Process

Printing methods also have implementation challenges in some aspects. While applying DIW requires strict rheology and limits resolution, small nozzles and slow extrusion speeds could improve alignment, but slow throughput and clogging are common obstacles. Adjusting speed, temperature, nozzle diameter, and layer height could influence alignment and actuation. Slow speeds (2–3 mm s^{-1}) ensure bonding and surface quality; high speeds increase shrinkage, but can also impair extrusion and actuation. The variation in the print path, such as alternating by 0° or 90° layers, could also change bending modes [107].

VP methods (DLP, TPP) provide sub-micron level resolution but require surface anchoring or magnetic fields to orient mesogens in a specific direction; finite anchoring restricts alignment to thin layers, less than 100 µm, and strong fields or patterned substrates reduce scalability. Multiphoton lithography is a slow process. Embedded printing allows free-form shapes, but manufacturing complex 3D structures with rapid actuation is still challenging [10].

Shape programming adds another layer of complexity to the process. For the DIW process, achieving multiaxis orientation from uniaxial alignment along the print path requires multistep printing or post-processing (stretching, fields, or patterning). Predictive models and finite-element simulations still have room for improvement. The model validation process could be improved by in situ monitoring of viscosity, phase state, and alignment using rheometry, birefringence, or scattering techniques. Integrated monitoring of printing parameters could enable feedback control for consistent performance during the manufacturing of complex geometries.

6.1.2. Challenges for Soft Robotic Actuators

Soft robotics utilizes compliant materials for lifelike motion. LCEs can deliver large strains (almost 40%) and moderate stresses (10 MPa), and photopolymerized networks can even achieve contractile stresses close to 270 kPa [71]. Yet thermotropic LCEs require heating in the range of 60 to 100 °C, demanding heaters or light sources and raising energy and thermal management concerns; also, cooling inhibits cycle frequency [108]. UV/blue light activation creates probable causes of degradation. Photothermal nanoparticles improve efficiency but may aggregate and undergo phase separation [106]. Continuous fiber reinforcement can boost blocking stress, but the printing procedure is very complicated [83].

Durability is another issue for LCEs: lightly cross-linked networks are prone to fatigue, and many actuators operate for fewer than 100 cycles [106]. Tethered power or external heating increases weight and stiffness. Recent innovations enable coaxial DIW of LCEs with liquid-metal cores for Joule heating and sensing [76]. While multimaterial printing can deposit stretchable Ag–EGaIn circuits on LCE surfaces [80,109], integrating electronics while maintaining compliance is challenging. DIW-printed monodomain LCE lattices dissipate energy across broad strain rates, though producing macroscopically aligned structures is hampered by complex chemistries [110]. Overall, improvements are needed in speed, efficiency, fatigue life, integrated power and sensing, and 3D programming.

6.1.3. Challenges for Biomedical Applications

LCEs are also vital elements in adaptive implants, scaffolds, and sensors. To ensure safety and long-term performance, LCE devices require thorough in vitro and in vivo

testing [111]. They also need to maintain stability under physiological conditions (temperature around 37 °C, neutral pH, and biochemical exposure) [112]. Potential degradation or monomer leaching can cause inflammatory responses or loss of function, so interfaces must be designed to adhere to tissues without irritation, and hydrophobic surfaces may need coatings to enhance cell compatibility. Aligning the mechanical properties of LCEs to those of surrounding tissues is crucial: materials that are too stiff could generate stress, while those that are too soft may not transmit force effectively. Some partially cross-linked LCEs, which allow spatial orientation, may lack long-term robustness [113]. Advances in biocompatible and biodegradable inks, derived from bio-based monomers and hydrogels, are beginning to address these issues [114].

6.2. Future Perspectives

The progress of LCE manufacturing by 4D printing is dependent on improvements in materials, printing, and device integration. Expanding beyond synthesis from acrylates is vital since epoxide mesogens reduce shrinkage and oxygen sensitivity [45], while dynamic covalent chemistries promise self-healing. Supramolecular networks offer reprocessability but currently have limited performance [105]. Stimuli-responsive cross-links could enable chemoresponsive or pH-sensitive actuation. Hierarchical composites pairing LCEs with conductive polymers, hydrogels, or shape-memory polymers may yield multimodal actuation. Low-temperature inks, which can operate at 63 °C and provide tunable actuation via temperature and speed adjustments [109], suggest that future materials should target lower transition temperatures.

Printing technologies also need significant advancement. DIW inks with larger processing windows would improve alignment and throughput. Modular print heads that can extrude multiple inks or fibers simultaneously could create dynamic director orientation. VP can benefit from patterning or flow-induced alignment to avoid external fields and achieve thicker part manufacturing. Hybrid DIW–DLP platforms, which are already capable of printing freestanding structures with active lattices, need further refinement; photothermal fillers yield light-responsive locomotion [115]. Real-time process monitoring using rheometry, birefringence, and thermography can improve feedback control systems, and in situ measurements of viscosity and alignment can complement modeling; density functional theory (DFT) and numerical simulations based on Computational fluid dynamics (CFD) using structured and unstructured meshes analyze polymerization and flow better from a theoretical perspective, while finite element analysis predicts deformation and optimizes design [116].

Looking ahead, interdisciplinary efforts must bridge material design, modeling, and engineering. Soft-robotic actuators require high efficiency and rapid cooling, potentially achieved through conductive fillers or embedded channels. Hybrid energy sources, Joule heating, photothermal, and magnetic, can enable multimodal control. Untethered operation will need lightweight batteries, photonic waveguides or wireless power. Biomedical devices demand biocompatible inks, sterilization, and long-term stability, plus interfaces that respond to cell signals. Nanomaterial additives can enhance mechanics and functionality, acting as rheology modifiers, mechanical enhancers and functional agents [117]. Beyond actuation, DIW-printed monodomain LCE lattices may offer mechanical damping across diverse strain rates despite alignment challenges [110], and cholesteric LCEs could enable stretchable photonic devices. The convergence of material innovation, advanced printing and integrated devices will unlock the transformative potential of LCEs in soft robotics and biomedicine.

7. Conclusions

The convergence of LCEs and 4D printing represents a transformative step in advanced manufacturing of shape-morphing materials that unite programmable mechanics, stimuli responsiveness, and structural intelligence. Over the past decade, several significant advancements have defined this domain, including shear-induced mesogen alignment through DIW, which established a direct route for encoding molecular orientation and achieving reversible actuation strains that exceed those by almost 50%, and orientation or functional gradient printing, which enabled complex and multimodal shape transformations. Dynamic covalent and thiol–Michael chemistries enabled the development of reconfigurable, self-healing, and recyclable LCE networks, which would extend device lifespan and sustainability. Meanwhile, VP methods such as DLP and TPP facilitated submicron precision and voxel-level mesogen alignment, bridging macroscale actuation and microscale photonics. In addition, hybrid and multimaterial integrations, including conductive and fiber-reinforced composites, have advanced load capacity, actuation efficiency, and functionality through the incorporation of electrothermal heating and sensing capabilities. The translation of these advances into biomedical technologies, from adaptive scaffolds and morphing implants to near-ambient-temperature wearable systems, highlights the growing potential of 4D-printed LCEs in patient-specific and minimally invasive applications. Despite remarkable achievements so far, challenges persist in print resolution of the objects, scalability, long-term durability, and biocompatibility. Ink formulations are constrained by mesogen alignment and synthesis limitations, as well as narrow rheological windows, while printing precision and multiaxial alignment require advanced process regulation. For biomedical applications, ensuring mechanical compatibility, bio-safety, and long-term stability under physiological conditions remains essential. Looking forward, innovation will hinge on developing low-temperature, biocompatible, and recyclable LCE inks, as well as hybrid additive platforms that integrate DIW, DLP, or DLW-TPP techniques with alignment control via magnetic induction, and in situ monitoring systems that link molecular alignment to macroscopic actuation. For applications in actuation, focus has been given on the active mechanical performance of the 4D-printed LCE objects. However, in addition, integration of Artificial Intelligence would be very beneficial for performance optimization and overall improvement of the manufacturing process. The fusion of materials chemistry, numerical simulation, physics-based modeling, and process development will enable reconfigurable, autonomous, and multifunctional systems, positioning 4D-printed LCEs at the forefront of next-generation research endeavors.

Author Contributions: Conceptualization, M.H. and Y.L.; methodology, M.H.; software, M.H.; validation, M.H. and Y.L.; formal analysis, M.H.; investigation, M.H.; resources, M.H.; data curation, M.H.; writing—original draft preparation, M.H.; writing—review and editing, M.H.; visualization, M.H.; supervision, Y.L.; project administration, Y.L.; funding acquisition, Y.L. All authors have read and agreed to the published version of the manuscript.

Funding: This research received no external funding.

Institutional Review Board Statement: Not applicable.

Data Availability Statement: No new data were created or analyzed in this study. Data sharing is not applicable to this article.

Conflicts of Interest: The authors declare no conflicts of interest.

Abbreviations

The following abbreviations are used in this manuscript:

CFD	Computational Fluid Dynamics
CNC	Cellulose Nanocrystals
Ch-LCE	Cholesteric Liquid Crystal Elastomer
ECM	Extracellular Matrix
ELM	Engineered Living Material
DFT	Density Functional Theory
DIW	Direct Ink Writing
DLP	Digital Light Processing
FEM	Finite Element Method
LC	Liquid Crystal
LCE	Liquid Crystal Elastomer
LCN	Liquid Crystal Network
NAT-LCE	Near-Ambient Temperature-Responsive Liquid Crystal Elastomer
PDMS	Polydimethylsiloxane
PEI	Polyethyleneimine
RM	Reactive Mesogen
SLA	Stereolithography
TPP	Two-Photon Polymerization
VP	Vat Photopolymerization

References

1. Thomsen, D.L.; Keller, P.; Naciri, J.; Pink, R.; Jeon, H.; Shenoy, D.; Ratna, B.R. Liquid Crystal Elastomers with Mechanical Properties of a Muscle. *Macromolecules* **2001**, *34*, 5868–5875. [CrossRef]
2. Camacho-Lopez, M.; Finkelmann, H.; Palffy-Muhoray, P.; Shelley, M. Fast Liquid-Crystal Elastomer Swims into the Dark. *Nat. Mater.* **2004**, *3*, 307–310. [CrossRef]
3. Warner, M.; Modes, C.D.; Corbett, D. Curvature in Nematic Elastica Responding to Light and Heat. *Proc. R. Soc. Math. Phys. Eng. Sci.* **2010**, *466*, 2975–2989. [CrossRef]
4. Zang, T.; Fu, S.; Cheng, J.; Zhang, C.; Lu, X.; Hu, J.; Xia, H.; Zhao, Y. 4D Printing of Shape-Morphing Liquid Crystal Elastomers. *Chem Bio Eng.* **2024**, *1*, 488–515. [CrossRef]
5. Zhang, C.; Lu, X.; Fei, G.; Wang, Z.; Xia, H.; Zhao, Y. 4D Printing of a Liquid Crystal Elastomer with a Controllable Orientation Gradient. *ACS Appl. Mater. Interfaces* **2019**, *11*, 44774–44782. [CrossRef]
6. Küpfer, J.; Finkelmann, H. Nematic Liquid Single Crystal Elastomers. *Makromol. Chem. Rapid Commun.* **1991**, *12*, 717–726. [CrossRef]
7. Herbert, K.M.; Fowler, H.E.; McCracken, J.M.; Schlafmann, K.R.; Koch, J.A.; White, T.J. Synthesis and Alignment of Liquid Crystalline Elastomers. *Nat. Rev. Mater.* **2022**, *7*, 23–38. [CrossRef]
8. Bodaghi, M.; Wang, L.; Zhang, F.; Liu, Y.; Leng, J.; Xing, R.; Dickey, M.D.; Vanaei, S.; Elahinia, M.; Hoa, S.V.; et al. 4D Printing Roadmap. *Smart Mater. Struct.* **2024**, *33*, 113501. [CrossRef]
9. Zhao, C.; Lv, Q.; Wu, W. Application and Prospects of Hydrogel Additive Manufacturing. *Gels* **2022**, *8*, 297. [CrossRef] [PubMed]
10. McDougall, L.; Herman, J.; Huntley, E.; Leguizamon, S.; Cook, A.; White, T.; Kaehr, B.; Roach, D.J. Free-Form Liquid Crystal Elastomers via Embedded 4D Printing. *ACS Appl. Mater. Interfaces* **2023**, *15*, 58897–58904. [CrossRef]
11. Huang, T.-Y.; Huang, H.-W.; Jin, D.D.; Chen, Q.Y.; Huang, J.Y.; Zhang, L.; Duan, H.L. Four-Dimensional Micro-Building Blocks. *Sci. Adv.* **2020**, *6*, eaav8219. [CrossRef] [PubMed]
12. Zhu, C.; Lu, Y.; Jiang, L.; Yu, Y. Liquid Crystal Soft Actuators and Robots toward Mixed Reality. *Adv. Funct. Mater.* **2021**, *31*, 2009835. [CrossRef]
13. He, Z.; Tan, G.; Chanda, D.; Wu, S.-T. Novel Liquid Crystal Photonic Devices Enabled by Two-Photon Polymerization [Invited]. *Opt. Express* **2019**, *27*, 11472–11491. [CrossRef]
14. Hasan, M.; Sakib, M.N.; Sabroj, R.B.; Rahman, M.Z. 7.03—Advanced Nanomaterial-Based Biosensors for Clinical Diagnosis, Environmental Protection and Industrial Fermentation. In *Comprehensive Materials Processing*, 2nd ed.; Hashmi, S., Ed.; Elsevier: Oxford, UK, 2024; pp. 30–47, ISBN 978-0-323-96021-2.
15. Shiralipour, F.; Nik Akhtar, Y.; Gilmor, A.; Pegorin, G.; Valerio-Aguilar, A.; Hegmann, E. The Role of Liquid Crystal Elastomers in Pioneering Biological Applications. *Crystals* **2024**, *14*, 859. [CrossRef]

16. Warner, M.; Terentjev, E.M. *Liquid Crystal Elastomers*; International Series of Monographs on Physics; Oxford University Press: Oxford, UK, 2003; ISBN 978-0-19-852767-1.
17. de Gennes, P.-G. Un Muscle Artificiel Semi-Rapide. *Comptes Rendus Académie Sci. Ser. IIB Mech. Phys. Chem. Astron.* **1997**, *324*, 343–348. [CrossRef]
18. Brannum, M.T.; Steele, A.M.; Venetos, M.C.; Korley, L.T.J.; Wnek, G.E.; White, T.J. Light Control with Liquid Crystalline Elastomers. *Adv. Opt. Mater.* **2019**, *7*, 1801683. [CrossRef]
19. Ferrantini, C.; Pioner, J.M.; Martella, D.; Coppini, R.; Piroddi, N.; Paoli, P.; Calamai, M.; Pavone, F.S.; Wiersma, D.S.; Tesi, C.; et al. Development of Light-Responsive Liquid Crystalline Elastomers to Assist Cardiac Contraction. *Circ. Res.* **2019**, *124*, e44–e54. [CrossRef]
20. Iseki, S. *U.S. Patent Application No. 16/070555*; Liquid Crystalline Elastomer Precursor and Liquid Crystalline Elastomer; The United States Patent and Trademark Office (USPTO): Alexandria, VA, USA, 2019.
21. Hussain, M.; Jull, E.I.L.; Mandle, R.J.; Raistrick, T.; Hine, P.J.; Gleeson, H.F. Liquid Crystal Elastomers for Biological Applications. *Nanomaterials* **2021**, *11*, 813. [CrossRef]
22. Rešetič, A. Shape Programming of Liquid Crystal Elastomers. *Commun. Chem.* **2024**, *7*, 56. [CrossRef]
23. Wermter, H.; Finkelmann, H. Liquid Crystalline Elastomers as Artificial Muscles. *E-Polym.* **2001**, *1*. [CrossRef]
24. Terentjev, E.M. Liquid Crystal Elastomers: 30 Years After. *Macromolecules* **2025**, *58*, 2792–2806. [CrossRef] [PubMed]
25. Liu, C.; Qin, H.; Mather, P.T. Review of Progress in Shape-Memory Polymers. *J. Mater. Chem.* **2007**, *17*, 1543–1558. [CrossRef]
26. Dayyoub, T.; Maksimkin, A.V.; Filippova, O.V.; Tcherdyntsev, V.V.; Telyshev, D.V. Shape Memory Polymers as Smart Materials: A Review. *Polymers* **2022**, *14*, 3511. [CrossRef]
27. Jiang, Z.-C.; Liu, Q.; Xiao, Y.-Y.; Zhao, Y. Liquid Crystal Elastomers for Actuation: A Perspective on Structure-Property-Function Relation. *Prog. Polym. Sci.* **2024**, *153*, 101829. [CrossRef]
28. Li, Y.; Liu, T.; Ambrogi, V.; Rios, O.; Xia, M.; He, W.; Yang, Z. Liquid Crystalline Elastomers Based on Click Chemistry. *ACS Appl. Mater. Interfaces* **2022**, *14*, 14842–14858. [CrossRef]
29. Ware, T.H.; McConney, M.E.; Wie, J.J.; Tondiglia, V.P.; White, T.J. Voxelated Liquid Crystal Elastomers. *Science* **2015**, *347*, 982–984. [CrossRef]
30. Yakacki, C.M.; Saed, M.; Nair, D.P.; Gong, T.; Reed, S.M.; Bowman, C.N. Tailorable and Programmable Liquid-Crystalline Elastomers Using a Two-Stage Thiol–Acrylate Reaction. *RSC Adv.* **2015**, *5*, 18997–19001. [CrossRef]
31. Kotikian, A.; Truby, R.L.; Boley, J.W.; White, T.J.; Lewis, J.A. 3D Printing of Liquid Crystal Elastomeric Actuators with Spatially Programed Nematic Order. *Adv. Mater.* **2018**, *30*, 1706164. [CrossRef]
32. Ambulo, C.P.; Burroughs, J.J.; Boothby, J.M.; Kim, H.; Shankar, M.R.; Ware, T.H. Four-Dimensional Printing of Liquid Crystal Elastomers. *ACS Appl. Mater. Interfaces* **2017**, *9*, 37332–37339. [CrossRef]
33. López-Valdeolivas, M.; Liu, D.; Broer, D.J.; Sánchez-Somolinos, C. 4D Printed Actuators with Soft-Robotic Functions. *Macromol. Rapid Commun.* **2018**, *39*, 1700710. [CrossRef]
34. Kloxin, C.J.; Bowman, C.N. Covalent Adaptable Networks: Smart, Reconfigurable and Responsive Network Systems. *Chem. Soc. Rev.* **2013**, *42*, 7161–7173. [CrossRef]
35. Pei, Z.; Yang, Y.; Chen, Q.; Terentjev, E.M.; Wei, Y.; Ji, Y. Mouldable Liquid-Crystalline Elastomer Actuators with Exchangeable Covalent Bonds. *Nat. Mater.* **2014**, *13*, 36–41. [CrossRef] [PubMed]
36. Saed, M.O.; Gablier, A.; Terentejv, E.M. Liquid Crystalline Vitrimers with Full or Partial Boronic-Ester Bond Exchange. *Adv. Funct. Mater.* **2020**, *30*, 1906458. [CrossRef]
37. Saed, M.O.; Gablier, A.; Terentjev, E.M. Exchangeable Liquid Crystalline Elastomers and Their Applications. *Chem. Rev.* **2022**, *122*, 4927–4945. [CrossRef] [PubMed]
38. Barnes, M.; Verduzco, R. Direct Shape Programming of Liquid Crystal Elastomers. *Soft Matter* **2019**, *15*, 870–879. [CrossRef] [PubMed]
39. Harris, K.D.; Cuypers, R.; Scheibe, P.; van Oosten, C.L.; Bastiaansen, C.W.M.; Lub, J.; Broer, D.J. Large Amplitude Light-Induced Motion in High Elastic Modulus Polymer Actuators. *J. Mater. Chem.* **2005**, *15*, 5043–5048. [CrossRef]
40. Ni, B.; Liu, G.; Zhang, M.; Tatoulian, M.; Keller, P.; Li, M.-H. Customizable Sophisticated Three-Dimensional Shape Changes of Large-Size Liquid Crystal Elastomer Actuators. *ACS Appl. Mater. Interfaces* **2021**, *13*, 54439–54446. [CrossRef]
41. Tabrizi, M.; Ware, T.H.; Shankar, M.R. Voxelated Molecular Patterning in Three-Dimensional Freeforms. *ACS Appl. Mater. Interfaces* **2019**, *11*, 28236–28245. [CrossRef]
42. Münchinger, A.; Hahn, V.; Beutel, D.; Woska, S.; Monti, J.; Rockstuhl, C.; Blasco, E.; Wegener, M. Multi-Photon 4D Printing of Complex Liquid Crystalline Microstructures by In Situ Alignment Using Electric Fields. *Adv. Mater. Technol.* **2022**, *7*, 2100944. [CrossRef]
43. Yang, G.-Z.; Full, R.J.; Jacobstein, N.; Fischer, P.; Bellingham, J.; Choset, H.; Christensen, H.; Dario, P.; Nelson, B.J.; Taylor, R. Ten Robotics Technologies of the Year. *Sci. Robot.* **2019**, *4*, eaaw1826. [CrossRef]

44. Tan, L.J.; Zhu, W.; Zhou, K. Recent Progress on Polymer Materials for Additive Manufacturing. *Adv. Funct. Mater.* **2020**, *30*, 2003062. [CrossRef]
45. Chen, M.; Gao, M.; Bai, L.; Zheng, H.; Qi, H.J.; Zhou, K. Recent Advances in 4D Printing of Liquid Crystal Elastomers. *Adv. Mater.* **2023**, *35*, 2209566. [CrossRef] [PubMed]
46. Saadi, M.A.S.R.; Maguire, A.; Pottackal, N.T.; Thakur, M.S.H.; Ikram, M.M.; Hart, A.J.; Ajayan, P.M.; Rahman, M.M. Direct Ink Writing: A 3D Printing Technology for Diverse Materials. *Adv. Mater.* **2022**, *34*, 2108855. [CrossRef]
47. Ohm, C.; Serra, C.; Zentel, R. A Continuous Flow Synthesis of Micrometer-Sized Actuators from Liquid Crystalline Elastomers. *Adv. Mater.* **2009**, *21*, 4859–4862. [CrossRef]
48. Ligon, S.C.; Liska, R.; Stampfl, J.; Gurr, M.; Mülhaupt, R. Polymers for 3D Printing and Customized Additive Manufacturing. *Chem. Rev.* **2017**, *117*, 10212–10290. [CrossRef]
49. Wang, Z.; Wang, Z.; Zheng, Y.; He, Q.; Wang, Y.; Cai, S. Three-Dimensional Printing of Functionally Graded Liquid Crystal Elastomer. *Sci. Adv.* **2020**, *6*, eabc0034. [CrossRef]
50. Ren, L.; Li, B.; He, Y.; Song, Z.; Zhou, X.; Liu, Q.; Ren, L. Programming Shape-Morphing Behavior of Liquid Crystal Elastomers via Parameter-Encoded 4D Printing. *ACS Appl. Mater. Interfaces* **2020**, *12*, 15562–15572. [CrossRef] [PubMed]
51. del Pozo Puig, M.; Sol, J.A.H.P.; van Uden, S.H.P.; Peeketi, A.R.; Lugger, S.J.D.; Annabattula, R.K.; Schenning, A.P.H.J.; Debije, M.G. Patterned Actuators via Direct Ink Writing of Liquid Crystals. *ACS Appl. Mater. Interfaces* **2021**, *13*, 59381–59391. [CrossRef] [PubMed]
52. Liu, J.; Gao, Y.; Wang, H.; Poling-Skutvik, R.; Osuji, C.O.; Yang, S. Shaping and Locomotion of Soft Robots Using Filament Actuators Made from Liquid Crystal Elastomer–Carbon Nanotube Composites. *Adv. Intell. Syst.* **2020**, *2*, 1900163. [CrossRef]
53. del Pozo, M.; Sol, J.A.H.P.; Schenning, A.P.H.J.; Debije, M.G. 4D Printing of Liquid Crystals: What's Right for Me? *Adv. Mater.* **2022**, *34*, 2104390. [CrossRef]
54. Gantenbein, S.; Masania, K.; Woigk, W.; Sesseg, J.P.W.; Tervoort, T.A.; Studart, A.R. Three-Dimensional Printing of Hierarchical Liquid-Crystal-Polymer Structures. *Nature* **2018**, *561*, 226–230. [CrossRef]
55. Naciri, J.; Srinivasan, A.; Jeon, H.; Nikolov, N.; Keller, P.; Ratna, B.R. Nematic Elastomer Fiber Actuator. *Macromolecules* **2003**, *36*, 8499–8505. [CrossRef]
56. Controlled Microstructural Architectures Based on Smart Fabrication Strategies - Ding - 2020 - Advanced Functional Materials - Wiley Online Library. Available online: https://advanced-onlinelibrary-wiley-com.ezproxy.lib.ou.edu/doi/full/10.1002/adfm.201901760 (accessed on 4 September 2025).
57. Pagac, M.; Hajnys, J.; Ma, Q.-P.; Jancar, L.; Jansa, J.; Stefek, P.; Mesicek, J. A Review of Vat Photopolymerization Technology: Materials, Applications, Challenges, and Future Trends of 3D Printing. *Polymers* **2021**, *13*, 598. [CrossRef]
58. The Recent Development of Vat Photopolymerization: A Review | Request PDF. Available online: https://www.researchgate.net/publication/355727288_The_recent_development_of_vat_photopolymerization_A_review (accessed on 4 September 2025).
59. Multimaterial Vat Polymerization Additive Manufacturing. Available online: https://colab.ws/articles/10.1021%2Facsapm.1c00262 (accessed on 4 September 2025).
60. Broer, D.J. On the History of Reactive Mesogens: Interview with Dirk J. Broer. *Adv. Mater.* **2020**, *32*, 1905144. [CrossRef]
61. Saha, S.K.; Wang, D.; Nguyen, V.H.; Chang, Y.; Oakdale, J.S.; Chen, S.-C. Scalable Submicrometer Additive Manufacturing. *Science* **2019**, *366*, 105–109. [CrossRef]
62. Ge, Q.; Chen, Z.; Cheng, J.; Zhang, B.; Zhang, Y.-F.; Li, H.; He, X.; Yuan, C.; Liu, J.; Magdassi, S.; et al. 3D Printing of Highly Stretchable Hydrogel with Diverse UV Curable Polymers. *Sci. Adv.* **2021**, *7*, eaba4261. [CrossRef] [PubMed]
63. Yu, C.; Schimelman, J.; Wang, P.; Miller, K.L.; Ma, X.; You, S.; Guan, J.; Sun, B.; Zhu, W.; Chen, S. Photopolymerizable Biomaterials and Light-Based 3D Printing Strategies for Biomedical Applications. *Chem. Rev.* **2020**, *120*, 10695–10743. [CrossRef]
64. Chen, L.; Zhang, Y.; Ye, H.; Duan, G.; Duan, H.; Ge, Q.; Wang, Z. Color-Changeable Four-Dimensional Printing Enabled with Ultraviolet-Curable and Thermochromic Shape Memory Polymers. *ACS Appl. Mater. Interfaces* **2021**, *13*, 18120–18127. [CrossRef]
65. Zeng, H.; Wasylczyk, P.; Cerretti, G.; Martella, D.; Parmeggiani, C.; Wiersma, D.S. Alignment Engineering in Liquid Crystalline Elastomers: Free-Form Microstructures with Multiple Functionalities. *Appl. Phys. Lett.* **2015**, *106*, 111902. [CrossRef]
66. Lin, J.-D.; Daniel Ho, Y.-L.; Chen, L.; Lopez-Garcia, M.; Jiang, S.-A.; Taverne, M.P.C.; Lee, C.-R.; Rarity, J.G. Microstructure-Stabilized Blue Phase Liquid Crystals. *ACS Omega* **2018**, *3*, 15435–15441. [CrossRef]
67. He, Z.; Lee, Y.-H.; Chen, R.; Chanda, D.; Wu, S.-T. Switchable Pancharatnam–Berry Microlens Array with Nano-Imprinted Liquid Crystal Alignment. *Opt. Lett.* **2018**, *43*, 5062–5065. [CrossRef]
68. Serra, F.; Eaton, S.M.; Cerbino, R.; Buscaglia, M.; Cerullo, G.; Osellame, R.; Bellini, T. Nematic Liquid Crystals Embedded in Cubic Microlattices: Memory Effects and Bistable Pixels. *Adv. Funct. Mater.* **2013**, *23*, 3990–3994. [CrossRef]
69. Sungur, E.; Li, M.-H.; Taupier, G.; Boeglin, A.; Romeo, M.; Méry, S.; Keller, P.; Dorkenoo, K.D. External Stimulus Driven Variable-Step Grating in a Nematic Elastomer. *Opt. Express* **2007**, *15*, 6784–6789. [CrossRef] [PubMed]

70. McCracken, J.M.; Tondiglia, V.P.; Auguste, A.D.; Godman, N.P.; Donovan, B.R.; Bagnall, B.N.; Fowler, H.E.; Baxter, C.M.; Matavulj, V.; Berrigan, J.D.; et al. Microstructured Photopolymerization of Liquid Crystalline Elastomers in Oxygen-Rich Environments. *Adv. Funct. Mater.* **2019**, *29*, 1903761. [CrossRef]
71. Li, S.; Bai, H.; Liu, Z.; Zhang, X.; Huang, C.; Wiesner, L.W.; Silberstein, M.; Shepherd, R.F. Digital Light Processing of Liquid Crystal Elastomers for Self-Sensing Artificial Muscles. *Sci. Adv.* **2021**, *7*, eabg3677. [CrossRef] [PubMed]
72. Chen, G.; Jin, B.; Shi, Y.; Zhao, Q.; Shen, Y.; Xie, T. Rapidly and Repeatedly Reprogrammable Liquid Crystalline Elastomer via a Shape Memory Mechanism. *Adv. Mater.* **2022**, *34*, 2201679. [CrossRef]
73. Yuan, C.; Roach, D.J.; Dunn, C.K.; Mu, Q.; Kuang, X.; Yakacki, C.M.; Wang, T.J.; Yu, K.; Qi, H.J. 3D Printed Reversible Shape Changing Soft Actuators Assisted by Liquid Crystal Elastomers. *Soft Matter* **2017**, *13*, 5558–5568. [CrossRef]
74. Zhang, D.; Tian, X.; Zhou, Y.; Li, D. 4D-Printed Fiber-Reinforced Liquid Crystal Elastomer Composites for Multifunctional Soft Robots with Self-Heating Actuation. *Virtual Phys. Prototyp.* **2025**, *20*, e2499927. [CrossRef]
75. Luo, C.; Chung, C.; Traugutt, N.A.; Yakacki, C.M.; Long, K.N.; Yu, K. 3D Printing of Liquid Crystal Elastomer Foams for Enhanced Energy Dissipation Under Mechanical Insult. *ACS Appl. Mater. Interfaces* **2020**, *13*. [CrossRef]
76. Kotikian, A.; Morales, J.M.; Lu, A.; Mueller, J.; Davidson, Z.S.; Boley, J.W.; Lewis, J.A. Innervated, Self-Sensing Liquid Crystal Elastomer Actuators with Closed Loop Control. *Adv. Mater.* **2021**, *33*, 2101814. [CrossRef]
77. Song, X.; Zhang, W.; Liu, H.; Zhao, L.; Chen, Q.; Tian, H. 3D Printing of Liquid Crystal Elastomers-Based Actuator for an Inchworm-Inspired Crawling Soft Robot. *Front. Robot. AI* **2022**, *9*. [CrossRef] [PubMed]
78. Wang, Y.; Yin, R.; Jin, L.; Liu, M.; Gao, Y.; Raney, J.; Yang, S. 3D-Printed Photoresponsive Liquid Crystal Elastomer Composites for Free-Form Actuation. *Adv. Funct. Mater.* **2023**, *33*, 2210614. [CrossRef]
79. Pluralizing Actuation Behavior of 3D Printable Liquid Crystal Elastomers via Polymerization Sequence Control | Science Advances. Available online: https://www.science.org/doi/10.1126/sciadv.adp4814 (accessed on 9 September 2025).
80. Vinciguerra, M.R.; Patel, D.K.; Zu, W.; Tavakoli, M.; Majidi, C.; Yao, L. Multimaterial Printing of Liquid Crystal Elastomers with Integrated Stretchable Electronics. *ACS Appl. Mater. Interfaces* **2023**, *15*, 24777–24787. [CrossRef]
81. Sgotti Veiga, J.; Reis Carneiro, M.; Molter, R.; Vinciguerra, M.; Yao, L.; Majidi, C.; Tavakoli, M. Toward Fully Printed Soft Actuators: UV-Assisted Printing of Liquid Crystal Elastomers and Biphasic Liquid Metal Conductors. *Adv. Mater. Technol.* **2023**, *8*, 2300144. [CrossRef]
82. Kotikian, A.; Watkins, A.A.; Bordiga, G.; Spielberg, A.; Davidson, Z.S.; Bertoldi, K.; Lewis, J.A. Liquid Crystal Elastomer Lattices with Thermally Programmable Deformation via Multi-Material 3D Printing. *Adv. Mater.* **2024**, *36*, 2310743. [CrossRef]
83. Jiang, H.; Chung, C.; Dunn, M.L.; Yu, K. 4D Printing of Liquid Crystal Elastomer Composites with Continuous Fiber Reinforcement. *Nat. Commun.* **2024**, *15*, 8491. [CrossRef]
84. Xia, Y.; Mu, T.; Guo, J.; Liu, Y.; Leng, J. Multifunctional Untethered Soft Machines Driven by 4D Printed Electrically Responsive Actuators. *ACS Appl. Mater. Interfaces* **2025**, *17*, 36059–36068. [CrossRef]
85. Yuan, L.-X.; Liu, C.-Y.; Yang, J.-P.; Wang, Z.-J. Soft Crawling and Flipping Robots Based on Liquid Metal-Liquid Crystal Elastomer Composites. *Chin. J. Polym. Sci.* **2025**, *43*, 588–596. [CrossRef]
86. Herman, J.A.; Telles, R.; Cook, C.C.; Leguizamon, S.C.; Lewis, J.A.; Kaehr, B.; White, T.J.; Roach, D.J. Digital Light Process 3D Printing of Magnetically Aligned Liquid Crystalline Elastomer Free–Forms. *Adv. Mater.* **2024**, *36*, 2414209. [CrossRef] [PubMed]
87. Gungor-Ozkerim, P.S.; Inci, I.; Zhang, Y.S.; Khademhosseini, A.; Dokmeci, M.R. Bioinks for 3D Bioprinting: An Overview. *Biomater. Sci.* **2018**, *6*, 915–946. [CrossRef]
88. Groll, J.; Boland, T.; Blunk, T.; Burdick, J.A.; Cho, D.-W.; Dalton, P.D.; Derby, B.; Forgacs, G.; Li, Q.; Mironov, V.A.; et al. Biofabrication: Reappraising the Definition of an Evolving Field. *Biofabrication* **2016**, *8*, 013001. [CrossRef]
89. Murphy, S.V.; Atala, A. 3D Bioprinting of Tissues and Organs. *Nat. Biotechnol.* **2014**, *32*, 773–785. [CrossRef]
90. Zhang, Y.S.; Yue, K.; Aleman, J.; Moghaddam, K.M.; Bakht, S.M.; Yang, J.; Jia, W.; Dell'Erba, V.; Assawes, P.; Shin, S.R.; et al. 3D Bioprinting for Tissue and Organ Fabrication. *Ann. Biomed. Eng.* **2017**, *45*, 148–163. [CrossRef] [PubMed]
91. Ustunel, S.; Sternbach, S.; Prévôt, M.E.; Freeman, E.J.; McDonough, J.A.; Clements, R.J.; Hegmann, E. 3D Co-Culturing of Human Neuroblastoma and Human Oligodendrocytes, Emulating Native Tissue Using 3D Porous Biodegradable Liquid Crystal Elastomers. *J. Appl. Polym. Sci.* **2023**, *140*, e53883. [CrossRef]
92. Saed, M.O.; Ambulo, C.P.; Kim, H.; De, R.; Raval, V.; Searles, K.; Siddiqui, D.A.; Cue, J.M.O.; Stefan, M.C.; Shankar, M.R.; et al. Molecularly-Engineered, 4D-Printed Liquid Crystal Elastomer Actuators. *Adv. Funct. Mater.* **2019**, *29*, 1806412. [CrossRef]
93. Davidson, E.C.; Kotikian, A.; Li, S.; Aizenberg, J.; Lewis, J.A. 3D Printable and Reconfigurable Liquid Crystal Elastomers with Light-Induced Shape Memory via Dynamic Bond Exchange. *Adv. Mater.* **2020**, *32*, 1905682. [CrossRef]
94. Volpe, R.H.; Mistry, D.; Patel, V.V.; Patel, R.R.; Yakacki, C.M. Dynamically Crystalizing Liquid-Crystal Elastomers for an Expandable Endplate-Conforming Interbody Fusion Cage. *Adv. Healthc. Mater.* **2020**, *9*, 1901136. [CrossRef]
95. Rivera-Tarazona, L.K.; Shukla, T.; Singh, K.A.; Gaharwar, A.K.; Campbell, Z.T.; Ware, T.H. 4D Printing of Engineered Living Materials. *Adv. Funct. Mater.* **2022**, *32*, 2106843. [CrossRef]

96. Sydney Gladman, A.; Matsumoto, E.A.; Nuzzo, R.G.; Mahadevan, L.; Lewis, J.A. Biomimetic 4D Printing. *Nat. Mater.* **2016**, *15*, 413–418. [CrossRef]
97. Li, D.X.; Yan, Y.D.; Oh, D.H.; Yang, K.Y.; Seo, Y.G.; Kim, J.O.; Kim, Y.-I.; Yong, C.S.; Choi, H.-G. Development of Valsartan-Loaded Gelatin Microcapsule without Crystal Change Using Hydroxypropylmethylcellulose as a Stabilizer. *Drug Deliv.* **2010**, *17*, 322–329. [CrossRef]
98. Dai, L.; Wang, L.; Chen, B.; Xu, Z.; Wang, Z.; Xiao, R. Shape Memory Behaviors of 3D Printed Liquid Crystal Elastomers. *Soft Sci.* **2023**, *3*, 5. [CrossRef]
99. Li, D.; Sun, Y.; Li, X.; Li, X.; Zhu, Z.; Sun, B.; Nong, S.; Wu, J.; Pan, T.; Li, W.; et al. 3D Printing of Near-Ambient Responsive Liquid Crystal Elastomers with Enhanced Nematic Order and Pluralized Transformation. *ACS Nano* **2025**, *19*, 7075–7087. [CrossRef]
100. He, Z.; Jiang, S.; Wang, J.; Attia, N.F.; Kang, D.; Zhou, G.; Xiao, S. Sweat Gland-Inspired Skin Soft Actuators of the Liquid Crystal Elastomer Enabled by 3D Printing. *Chem. Eng. J.* **2025**, *506*, 160261. [CrossRef]
101. Hou, W.; Wang, J.; Lv, J. Bioinspired Liquid Crystalline Spinning Enables Scalable Fabrication of High-Performing Fibrous Artificial Muscles. *Adv. Mater.* **2023**, *35*, 2211800. [CrossRef]
102. Roach, D.J.; Yuan, C.; Kuang, X.; Li, V.C.-F.; Blake, P.; Romero, M.L.; Hammel, I.; Yu, K.; Qi, H.J. Long Liquid Crystal Elastomer Fibers with Large Reversible Actuation Strains for Smart Textiles and Artificial Muscles. *ACS Appl. Mater. Interfaces* **2019**, *11*, 19514–19521. [CrossRef]
103. Sol, J.A.H.P.; Douma, R.F.; Schenning, A.P.H.J.; Debije, M.G. 4D Printed Light-Responsive Patterned Liquid Crystal Elastomer Actuators Using a Single Structural Color Ink. *Adv. Mater. Technol.* **2023**, *8*, 2200970. [CrossRef]
104. Prévôt, M.E.; Ustunel, S.; Freychet, G.; Webb, C.R.; Zhernenkov, M.; Pindak, R.; Clements, R.J.; Hegmann, E. Physical Models from Physical Templates Using Biocompatible Liquid Crystal Elastomers as Morphologically Programmable Inks For 3D Printing. *Macromol. Biosci.* **2023**, *23*, 2200343. [CrossRef]
105. Lugger, S.J.D.; Verbroekken, R.M.C.; Mulder, D.J.; Schenning, A.P.H.J. Direct Ink Writing of Recyclable Supramolecular Soft Actuators. *ACS Macro Letters* **2022**, *11*, 935–940. [CrossRef]
106. Sun, D.; Zhang, J.; Li, H.; Shi, Z.; Meng, Q.; Liu, S.; Chen, J.; Liu, X. Toward Application of Liquid Crystalline Elastomer for Smart Robotics: State of the Art and Challenges. *Polymers* **2021**, *13*, 1889. [CrossRef]
107. Li, S.; Song, Z.; Fan, Y.; Wei, D.; Liu, Y. Four-Dimensional Printing of Temperature-Responsive Liquid Crystal Elastomers with Programmable Shape-Changing Behavior. *Biomimetics* **2023**, *8*, 196. [CrossRef] [PubMed]
108. Wang, Z.; Wang, Y.; Cai, S.; Yang, J. Liquid Crystal Elastomers for Soft Actuators. *Mater. Lab* **2022**, *1*, 220030–220034. [CrossRef]
109. Warner, M. Topographic Mechanics and Applications of Liquid Crystalline Solids. *Annu. Rev. Condens. Matter Phys.* **2020**, *11*, 125–145. [CrossRef]
110. Bischoff, A.; Bawcutt, C.; Sorkin, M.; Yazzie, J.; Cook, C.; Leguizamon, S.C.; Cook, A.W.; Roach, D.J. Monodomain Liquid-Crystal Elastomer Lattices for Broad Strain-Rate Mechanical Damping. *Adv. Eng. Mater.* **2025**, *27*, 2401796. [CrossRef]
111. Zhang, Z.; Yang, X.; Zhao, Y.; Ye, F.; Shang, L. Liquid Crystal Materials for Biomedical Applications. *Adv. Mater.* **2023**, *35*, 2300220. [CrossRef] [PubMed]
112. Barnes, M.; Cetinkaya, S.; Ajnsztajn, A.; Verduzco, R. Understanding the Effect of Liquid Crystal Content on the Phase Behavior and Mechanical Properties of Liquid Crystal Elastomers. *Soft Matter* **2022**, *18*, 5074–5081. [CrossRef]
113. Ustunel, S.; Pandya, H.; Prévôt, M.E.; Pegorin, G.; Shiralipour, F.; Paul, R.; Clements, R.J.; Khabaz, F.; Hegmann, E. A Molecular Rheology Dynamics Study on 3D Printing of Liquid Crystal Elastomers. *Macromol. Rapid Commun.* **2024**, *45*, 2300717. [CrossRef]
114. Ambulo, C.P.; Tasmim, S.; Wang, S.; Abdelrahman, M.K.; Zimmern, P.E.; Ware, T.H. Processing Advances in Liquid Crystal Elastomers Provide a Path to Biomedical Applications. *J. Appl. Phys.* **2020**, *128*, 140901. [CrossRef]
115. Peng, X.; Wu, S.; Sun, X.; Yue, L.; Montgomery, S.M.; Demoly, F.; Zhou, K.; Zhao, R.R.; Qi, H.J. 4D Printing of Freestanding Liquid Crystal Elastomers via Hybrid Additive Manufacturing. *Adv. Mater.* **2022**, *34*. [CrossRef]
116. Razib, R.; Hasan, M.; Bhuiyan, S.A.; Kader, M.S. Numerical analysis of steady laminar flow by finite volume method in connection with simple algorithm 2023. In Proceedings of the 13th International Conference on Marine Technology (MARTEC 2022), Skudai, Malazia, 21–22 December 2022.
117. Guo, S.; Cui, H.; Agarwal, T.; Zhang, L.G. Nanomaterials in 4D Printing: Expanding the Frontiers of Advanced Manufacturing. *Small* **2024**, *20*, 2307750. [CrossRef] [PubMed]

Disclaimer/Publisher's Note: The statements, opinions and data contained in all publications are solely those of the individual author(s) and contributor(s) and not of MDPI and/or the editor(s). MDPI and/or the editor(s) disclaim responsibility for any injury to people or property resulting from any ideas, methods, instructions or products referred to in the content.